https://jksus.org

Journal of King Saud University – Science

Article in Press

Original Article

The dual role of bio-inspired palladium nanoparticles in antibacterial action and wound healing: An *in vitro* and *in vivo* study

Ashwini Singhal[a,#], Gyan Prakash Meghwal[b], Apurva Jaiswal[c,#], Neha Kaushik[d], Anita Kumari[a], Nighat Fahmi[a], Rizwan Wahab[e], Dev Dutt Patel[b], Abdulaziz A. Al-Khedhairy[e], Priyadarshi Meena[b,*], Nagendra Kumar Kaushik[c,*], Ramhari Meena[a,*]

[a]*Department of Chemistry, University of Rajasthan, Rajasthan-302004, India*
[b]*Department of Zoology, University of Rajasthan, Rajasthan-302004, India*
[c]*Plasma Bioscience Research Center, Department of Electrical and Biological Physics, Kwangwoon University, Seoul 01897, Republic of Korea*
[d]*Department of Biotechnology, College of Engineering, The University of Suwon, Hwaseong 18323, Republic of Korea*
[e]*Chair for DNA Research, Zoology Department, College of Science, King Saud University, Riyadh 11451, Saudi Arabia*
[#]*These authors equally contributed to this work.*

ARTICLE INFO

Keywords:
Antimicrobial
Antioxidant
Bio-inspired synthesis
Palladium nanoparticles
Plectranthusamboinicus
Wound healing

ABSTRACT

Nanoparticles have become essential in theragnostic applications due to their multi-functionality. However, conventionally synthesized nanoparticles are often limited by high production costs and moderate efficacy. To address these challenges, this study focuses on bio-inspired palladium nanoparticles (PdNPs), an entirely novel nanomaterial synthesized with the *Plectranthus amboinicus* leaf extract offering an economical, green, biocompatible, and stable substitute. To characterize biosynthesized PdNPs, Fourier-transform infrared spectroscopy (FTIR), X-ray diffraction (XRD), UV-Vis spectroscopy, energy-dispersive X-ray spectroscopy (EDS), field emission scanning electron microscopy (FESEM), high-resolution transmission electron microscopy (TEM), and zeta potential analysis were employed. The nanoparticles, measuring 5–40 nm, displayed diverse shapes (spherical, triangular, and rectangular), with XRD revealing a face-centered cubic (fcc) crystalline structure. The zeta potential value of -12.9 mV indicated high stability due to the surface charge of the PdNPs. Therapeutically, PdNPs exhibited broad-spectrum antibacterial activity, particularly against *E. coli* (14 ± 0.3 mm inhibition zone), along with potent antioxidants (71.41 ± 0.94%), anti-diabetic (77%), and anti-inflammatory (72%) properties. Remarkably, PdNPs-based ointments in a mouse excision wound model demonstrated a 74.76% wound closure within 10 days in a mouse model, with complete healing achieved by day 14. This study therefore underscores the broad applicability of PdNPs emphasizing its novelty and potential as a competitive alternative to conventional therapies making it ideal for numerous biomedical applications such as wound healing, tissue repair, dentistry, regenerative medicine, and biosensing platforms.

1. Introduction

Metal nanoparticles (MNPs), which involves a broad range of examples with at least one dimension between 1 and 100 nm, have become an appealing class of materials in recent years. MNPs have unique properties beneficial in various applications like industrial catalysis (Solomon *et al.*, 2024), food packaging (Joshi *et al.*, 2024), biosensing (Kumalasari *et al.*, 2024), batteries (J. Zheng *et al.*, 2024), superconductor systems (Atchaya and Meena Devi, 2024), medicine (Issaka *et al.*, 2024; Naser *et al.*, 2024; Panda *et al.*, 2021; Puri *et al.*, 2024; Todaria *et al.*, 2024; Q. Zheng *et al.*, 2024), and bacterial disinfection (Paul *et al.*, 2018). Palladium nanoparticles (PdNPs) have diverse applications due to their unique characteristics and catalytic activity (Lin *et al.*, 2023; Losada-Garcia *et al.*, 2022; Seku *et al.*, 2024; Vinnacombe-Willson *et al.*, 2023). PdNPs play a crucial role in the automobile industry specifically in catalytic converters by neutralizing harmful gases, including carbon monoxide, unburned hydrocarbons, and nitrogen oxides and turning them into less detrimental compounds (Aarzoo *et al.*, 2022). They also serve as catalysts in various organic syntheses and electro-catalysts in fuel cells to promote the oxidation and reduction reactions involved in electricity generation (Dhumal *et al.*, 2024; Shukla *et al.*, 2023). In water treatment, PdNPs remove impurities and minimize pollutants, such as chlorinated hydrocarbons and heavy metals (Arsiya *et al.*, 2017; Emam, 2022; Shokouhimehr *et al.*, 2019; Vijwani *et al.*, 2012). They use air purification devices to catch and neutralize pollutants, hazardous gases, and conductive inks for flexible and wearable electronics (Cai *et al.*, 2018; Chen *et al.*, 2011; Palliyarayil *et al.*, 2020). Palladium nanoparticles are functionalized and implemented in cancer therapy (Alinaghi *et al.*, 2024; Li *et al.*, 2024), drug delivery systems (Shanthi *et al.*, 2015), biosensors (Orzari *et al.*, 2024; Phuong *et al.*, 2024), imaging agents (Liu *et al.*, 2020; Nie *et al.*, 2014), and antimicrobial agents (Hamid *et al.*, 2024; Nie *et al.*, 2014).

***Corresponding authors**
E-mail addresses: kaushik.nagendra@kw.ac.kr (N. K. Kaushik), ramharichem@gmail.com (R. Meena), priyadarshi.jrf@gmail.com (P. Meena)

Received: 19 November, 2024 **Accepted:** 27 February, 2025 **Epub Ahead of Print:** 18 April, 2025

DOI: 10.25259/JKSUS_355_2024

Several approaches have been designed modified to synthesize MNPs including the widely adopted top-down and bottom-up techniques (Lin *et al.*, 2023; Vinnacombe-Willson *et al.*, 2023). Broadly divided into two primary categories, chemical and physical, each of these approaches has their pros and cons, and selecting one is influenced by some aspects, such as preferred nanoparticle properties, scalability, and intended applications (El-Khawaga *et al.*, 2023; Gupta *et al.*, 2023; Verma *et al.*, 2016). While these processes provide for the accurate regulation of nanoparticle size and morphology, they are energy-intensive and often generate hazardous by-products (Kumari *et al.*, 2023; Saleh and Fadillah, 2023). To address these limitations, green synthesis methods utilize biological agents such as biomass or organisms as eco-friendly reducing and stabilizing agents (C and T, 2024; Shahid-ul-Islam *et al.*, 2023). These strategies employ various microorganisms (viruses, bacteria, yeast, algae and fungi) and organisms (plants) to synthesize MNPs under mild reaction conditions, minimizing energy consumption and ecological impact (Arteaga-Castrejón *et al.*, 2024; Bokolia *et al.*, 2024; Karunakaran *et al.*, 2023; Verma *et al.*, 2022).

Despite these advanced relatively greener approaches, there is a critical need to explore greener and more sustainable synthesis methods for MNPs, which do not rely on energy-intensive chemical and physical techniques that produce hazardous by-products (Bokolia *et al.*, 2024) (Meena *et al.*, 2024). Bio-inspired methods that utilize plant extracts have become a green alternative to conventional techniques, leveraging phytochemicals, such as alkaloids, flavonoids, polyphenols, and terpenoids serving as naturally occurring stabilizing and reducing agents. These aid in the reduction of metal ions to generate nanoparticles without the need of synthetic reducing agents and act as capping agents, providing stability, preventing aggregation, and improving colloidal stability of the nanoparticles (O. Adeyemi *et al.*, 2022). It is considered environmentally benign because it does not require the use of noxious chemicals and solvents that are frequently used in traditional synthesis processes (Vijayaram *et al.*, 2024). Bio-inspired synthesis frequently occurs under mild conditions, such as reduced temperatures and air pressure. Compared to traditional methods, plant-based synthesis is cost-effective, environmentally benign, and biocompatible. Moreover, the resultant nanoparticles exhibit excellent therapeutic properties, including stability, permeability, and reduced toxicity (Huang *et al.*, 2024). Therefore, researchers continue investigating and developing new methods to make MNPs emergence more sustainable and environmentally friendly.

This study focuses on *Plectranthusamboinicus,* a perennial Solanaceae herb with a wide distribution in tropical and warm regions. It has a variety of cultural uses in traditional medicine. Diverse phytochemicals in the plant extract of *P. amboinicus*, such as carvacrol, thymol, flavonoids, triterpenoids, and rosmarinic acid, contribute to the herb's biological activities, including antimicrobial, anti-inflammatory, antiviral, antiepileptic, antitumorigenic, wound healing, and antioxidant effects ("Health-promoting properties of Plectranthus amboinicus: a comprehensive review," 2023; Nizar Ahamed *et al.*, 2023). The phytochemical composition of *P. amboinicus* has shown high therapeutic and nutritional properties, garnering significant interest from the pharmaceutical industries for its potential medicinal applications (Augustus *et al.*, 2024; Gupta *et al.*, 2024; Paramasivam *et al.*, 2020).

The primary objective of this research was therefore the development of a green synthesis technique to synthesize bioinspired PdNPs using alcoholic leaf extracts of *P. amboinicus*. By integrating the unique properties of PdNPs and *P. amboinicus*-derived phytochemicals, this study aimed to develop a multifunctional nanotherapeutic agent. The bio-inspired PdNPs were assessed for their antimicrobial, antioxidant, anti-diabetic, and anti-inflammatory activities, as well as their wound-healing efficacy in a mouse excision wound model. By utilizing the combined advantages of the MNPs and plant extract, this strategy aimed to establish the synthesized PdNPs as a promising candidate for multifaceted therapeutic applications.

2. Experimental section

2.1. Materials and characterization techniques

Before employing glassware for synthesis, it is correctly cleansed with aqua regia (a mixture of HCl and HNO_3 in a 3:1 ratio) followed by rinsing with double-distilled water. Palladium chloride ($PdCl_2$, 99.9%) procured from Sigma-Aldrich was applied without further processing. Analytical-grade chemicals and Milli-Q-grade water were used for all experiments. The leaves of *P. amboinicus* were harvested from the university nursery, University of Rajasthan, Jaipur, India. The UV-visible (UV-Vis) absorption spectra of biosynthesized PdNPs were measured using an Agilent Technology Cary 60 Visible spectrophotometer with wavelength of 200–800 nm. Fourier transform infrared (FTIR) spectra of PdNPs were recorded on a FT-IR Spectrum 2 (Perkin Elmer) in the 400-4000 cm^{-1} range. Energy-dispersive X-ray spectroscopy (EDS)-equipped field emission scanning electron microscopy (Apreo 2S Highvac, Thermofisher Scientific) was utilized to investigate the morphology and element mapping of PdNPs. Transmission electron microscopy (Tecnai G2 S-TWIN, 200KV) was used to examine the size. The zeta potential of the re-dispersed nanoparticles was assessed using a Zetasizer Nano ZSP (ZEN 5600). The X-ray diffraction (XRD) pattern of PdNPs was determined using XPERT PRO PANAlytical XRD.

2.2. Leaf extract preparation

The leaves of *P. amboinicus* were obtained from the university nursery on the university campus. The acquired leaves were cleansed with tap and distilled water to eliminate any impurities. The cleaned leaves were grated into little pieces. In a 500 mL conical flask, 40 g of the grated leaves were placed, and 200 mL of water was added (leaves: water = 1:5 ratio). The conical flask was placed at heating plate and heated at 70-80 °C until the water began to boil. The solution changed to a brown color during heating and was subsequently cooled after boiling. The extract was kept at room temperature for later use after being cooled and filtered through Whatman No.1 filter paper to separate the liquid component (leaf extract) from the solid plant material.

2.3. Synthesis of PdNPs

The procedure for synthesizing palladium nanoparticles (PdNPs) is as follows. For a 1 mM PdCl2 solution (100 mL), dissolve 0.0741 g of $PdCl_2$ in 90 mL of ultrapure water. While stirring on a hot magnetic stirrer, add 2–3 drops of HCl to the solution to ensure complete dissolution. Next, 10 mL of the leaf extract was added to 90 mL of the 1 mM $PdCl_2$ solution and stir the mixture at 80°C for 30 mins. The reaction solution was kept undisturbed until the color changed from yellow to black. After the color shift, the solution was left to stabilize the nanoparticles under static conditions for 48 hrs. Finally, the solid nanoparticles were then collected by centrifuging the reaction mixture for 10 mins at 6000 rpm and dispersed again in Milli-Q water. The centrifugation and scattering processes were performed twice to eliminate any remaining $PdCl_2$ and *P. amboinicus* leaves extract solution from the final product. Following collection, the nanoparticles were dried up in a hot air oven (Fig. 1).

2.4. Antibacterial efficacy of PdNPs

The Agar Well Diffusion approach was employed for the *in vitro* antibacterial assay. The individual test materials were diluted with

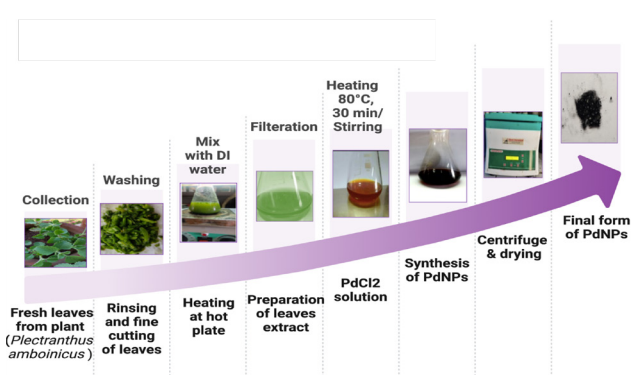

Fig. 1. Schematic diagram of the green synthesis of PdNPs using an aqueous extract of *P. amboinicus*. PdNPs: Palladium nanoparticles.

0.5% dimethyl sulphoxide (DMSO), and four varying concentrations (conc.) (25 μg/mL, 50 μg/mL, 75 μg/mL, and 100 μg/mL) of palladium chloride, *P. amboinicus* leaf extract, and PdNPs were created. Sterilized petri dishes containing the nutritional agar (NA) medium were employed to inoculate gram-negative and -positive bacterial strains including *Staphylococcus aureus (S. aureus), Bacillus subtilis (B. subtilis), and Escherichia coli (E. coli), Pseudomonas aeruginosa (P. aeruginosa), respectively*. This inoculum was spread evenly across the plate with a spreader and let to stand for 30 mins. Wells of 6 mm diameter were created in the seeded agar plates. A control well was also constructed at the same distance. All concentrations of palladium chloride, *P. amboinicus* leaf extract, PdNPs, and the standard medication (30 μg/mL) were poured into the pre-organized wells of seeded plates. The plates were incubated for 24 hrs at 37°C. The inhibition zone (IZ) around each well was employed to estimate the antibacterial spectrum of the test material. The sizes of the inhibition zones developed from the test samples and the commercial positive control (Streptomycin) were compared. The studies were carried out in triplicate, with the mean absorbance values reported.

2.5. Antioxidant activity of PdNPs

The efficiency of the PdNPs in scavenging DPPH radicals was compared to that of the standard ascorbic acid. For the experiment, 3 mL of a 0.1 mM DPPH solution in methanol was dissolved with variable conc. (20, 40, 60, 80, 100, 100, 150, 200, 250, 300, 500, and 1000 μg/mL) of palladium chloride, leaf extract, and synthesized PdNPs. The Mixture was agitated vigorously to achieve consistency and then kept for 30 mins in dark at an ambient temperature. The optical density was assessed at 517 nm using a UV-Vis spectrophotometer. The DPPH radical inhibition (%) was estimated using the following Eq. (1):

$$\%\text{DPPH radical inhibition} = \frac{A_{control} - A_{sample}}{A_{control}} \times 100 \quad (1)$$

The control samples's absorbance ($A_{control}$) and test sample's absorbance (A_{sample}) are key components in the formula for evaluating the DPPH radical inhibition. It's important to substitute the correct values of $A_{control}$ and A_{sample} into the formula to accurately determine the percentage of DPPH radical inhibition.

2.6. Anti-inflammatory activity of PdNPs

Anti-inflammatory activity was assessed employing a altered BSA method established by Williams *et al.* with varying conc. of 100, 250, 500, 1000, and 2000 μg/mL of aspirin and PdNPs (Williams *et al.*, 2002). A 0.4% w/v BSA solution was made by dissolving one Tris-buffered saline tablet in 15 mL deionized water, producing a buffer containing 0.05 M Tris and 0.15 M sodium chloride at pH 7.6 at 25°C. The pH was lowered to 6.4 using glacial acetic acid. PdNPs were dissolved in DMSO to prepare stock solutions at a concentration of 50 μg/mL (0.005% w/v). These PdNPs aliquots were mixed with 1 mL of 0.4% w/v BSA buffer in test tubes. The mixtures were incubated in a water bath at 72°C for 20 mins, followed by cooling for another 20 mins. A spectrophotometer was used to determine turbidity at 660 nm, with air serving as the blank. The studies were carried out in triplicate, with the mean absorbance values reported. The following formulae was used to determine the inhibition of BSA denaturation:

$$\text{Percentage inhibition of BAS Denaturation}(\%) = 100 \times \left(1 - \frac{A_1}{A_2}\right)$$

where A1 is the reference's absorbance and A2 is the sample's absorbance.

2.7. Anti-diabetic assay of PdNPs

The chromogenic DNSA method was employed in order to conduct an inhibition study. The assay solution contains 500 μL of 0.02 M sodium phosphate buffer (pH 6.9, supplemented with 6 mM NaCl), along with 1 mL of salivary amylase, and 400 μL test samples with conc. varying between 20 to 1000 μg/mL incubated for 10 mins at 37°C. Subsequently, 580 μL of a 1% w/v starch solution was added to each tube, followed by further incubation for 15 mins at 37°C. To terminate the reaction, 1.0 ml of DNSA reagent was added, followed by 5 mins in boiling water, cooling at room temperature, and OD measurement at 540 nm. The control without PdNPs had 100% enzymatic activity. Acarbose was added as a negative control along with the test sample in the reaction mix without any enzyme to remove the absorbance brought on by PdNPs. The percentage of alpha amylase inhibition was computed using the following:

$$\%\text{ Relative enzyme activity} = \frac{\text{Enzyme activity in test sample with PdNPs}}{\text{Enzyme activity in control}} \times 100$$

% Inhibition in the alpha-amylase activity = 100 - % Relative enzyme activity

2.8. Wound healing activity of PdNPs

2.8.1. Preparation PdNPs ointment

In order to formulate the ointment with PdNPs, 30 g of absolute Vaseline is heated in a water bath at 60°C using a bain-marie technique. Then, 0.3 g of PdNPs is added (1% w/w). Ultimately, the ointment that had been created undergoes sonication at 60°C for 30 mins in order to achieve a consistent and uniform texture (Zare-Bidaki *et al.*, 2023).

2.8.2. Animal care and handling

The mice (male Swiss albino mice) weighing 25–30 g were utilized in the present study. Animals were acquired from the Central Animal Facility (CAF) National Institute of Pharmaceutical Education and Research (NIPER), Mohali, Chandigarh (Reg. No: (108/GO/Re/Rc/Bi/Bt/99/CPCSEA). All animal experiment were approved from the Institutional Animal Ethical Committee, Department of Zoology, University of Rajasthan, Jaipur India letter no. UDZ/IAEC/V/07 dated 16-03-2022. Animals were kept in the animal house facility at the Department of Zoology, University of Rajasthan, Jaipur, during the experimental work. Polyacrylic cages were used to house the animals, ensuring standard conditions of 20–30°C temperature, 50–70% humidity, and a 12:12 light-to-dark cycle. A 7-day acclimation period was observed prior to the experiments, and the animals were fed dry pellets and tap water *ad libitum*. The study design for the wound healing potential of the biosynthesized PdNPs animals was divided into three groups as follows.

Group A: *Control Group:* - No treatment was administered to the animals in this group.

Group B: *Positive Control Group:* - Animals of this group were treated with Nitrofurazone (0.2%w/w) ointment

Group C: *Drug Treated Group:* - Animals of this group were treated with the Vaseline ointment containing PdNPs.

2.8.3. Excision wound model

Excisional wounds are widely used as a model for studying wound healing, as they closely mimic acute clinical wounds that heal by second intention, where the skin edges are left unsutured. The experimental procedure involved anesthetizing animals with diethyl ether, followed by shaving the dorsal back to prepare for a wound. Ethanol (70%) served as an antiseptic for the shaved area. A circular excision wound, extending through the full thickness of the skin, was then created on the predetermined shaved region without subsequent dressing. No local or systemic antimicrobial agents were administered. Each mouse was housed individually in a separate cage throughout the study. This methodology aimed to investigate the wound healing efficacy of the PdNPs without the interference of antimicrobial treatments, allowing for an assessment of natural recovery with and without drug treatment. Nitrofurazone (0.2%w/w) ointment was applied as a positive control.

2.8.4. Assessment of wound contraction

The experimental animals were divided into three groups following the production of wounds, as previously mentioned. The excision wound margins were traced via a clear plastic sheet, and the surface area of the wound was evaluated planimetrically. The size of wounds was measured in mm^2 by putting the transparent sheet on graph paper every day throughout the monitoring period; photographs of the dorsal surface of the mice were taken on the 1st, 6th, 12th, and 18th day. Wound contraction was estimated using the following formula:

$$\text{Percent wound contraction} = \frac{\text{Initial wound area-unhealed area}}{\text{Initial wound area}} \times 100$$

2.9. Statistical analysis

The experiment was carried out in three replicates for each treatment and overall results are presented as mean ± standard deviation. Student's t-test and one-way ANOVA were used to analyze the collected data. p-values < 0.05 imply statistical significance.

3. Results and discussion

3.1. UV−vis analysis of PdNPs

UV-vis spectroscopy is a common technique employed to characterize metal nanoparticles. The UV−vis absorbance of *P. amboinicus* leaves extract, $PdCl_2$ solution and bio-inspired synthesized PdNPs was observed within 200−800 nm wavelength. The reaction occurs between *P. amboinicus* leaves extract and $PdCl_2$; the reaction mixture's color shifts from yellow to black. The reaction mixture showed a dark brown color due to the stimulation of surface plasmon resonance (SPR) of PdNPs.UV-vis absorption spectra of the $PdCl_2$ solution showed a distinct absorption peak at 425 nm, revealing Pd (II) ions presence in the solution. After the reaction, the absorption peak at 425 nm of the precursor $PdCl_2$had disappeared, indicating that the precursor Pd (II) reduction was completed (Basavegowda *et al.*, 2015; Kuniyil *et al.*, 2019). Due to the surface Plasmon, PdNPs often do not exhibit any noticeable peaks (Fig. 2a).

3.2. FT-IR analysis of PdNPs

FT-IR spectroscopy is an incredibly effective analytical technique that reveals important information about chemical structures and functional groups. The FT-IR spectrum of the *P. amboinicus* leaves extract revealed important absorption peaks at 3420, 2925, 2853, 1617, 1430, 1385, 1078 and 617 cm^{-1} (Fig. 2(b), blue). *P. amboinicus* leaf extract's FTIR spectra showed absorption peaks at 3420 and 1617 cm^{-1}, indicating O−H and >C=C< stretching of flavonoids or polyols. The vibrations at 1078 and 1385 cm^{-1} were related to C–O stretching and the C–H bending of flavonoids or polyols. Additionally, the leaf extract displayed bands at 2925 and 2853 cm^{-1}, which corresponded to the C–H stretching vibrations mode of aliphatic compounds. In contrast, the FT-IR spectrum of PdNPs showed significant absorption peaks at 3372, 2920, 2820, 1560, 1410, 1342, 1024 and 648 cm^{-1}, clearly indicating the occurrence of phytoconstituents that serve as capping agents (Fig. 2(b), red). After the bio reduction of $PdCl_2$ by the leaf extract, there were noticeable modifications in the positions and intensity of the stretching vibrations, suggesting the involvement of polyphenols or flavonoids. The presence of the O–H group of polyols in the bio reduction process was confirmed by the band at 3372 cm^{-1}. Furthermore, the minor peaks at 2920 and 1560 cm^{-1} corresponded to C–H and C-O stretching vibrations, while the peaks at 1024 cm^{-1} were associated with the C–O stretching vibration in flavonoids or polyols (Dauthal and Mukhopadhyay, 2013; Jayamani *et al.*, 2023; Sarmah *et al.*, 2019).

3.3. X-ray diffraction analysis

The XRD diffractograms in Fig. 2(c) display the PdNPs synthesized through plant mediation. These diffractograms exhibit intense diffraction peaks at 2θ = 40.0, 46.4, 67.9, 81.8, and 86.5°, corresponding to the

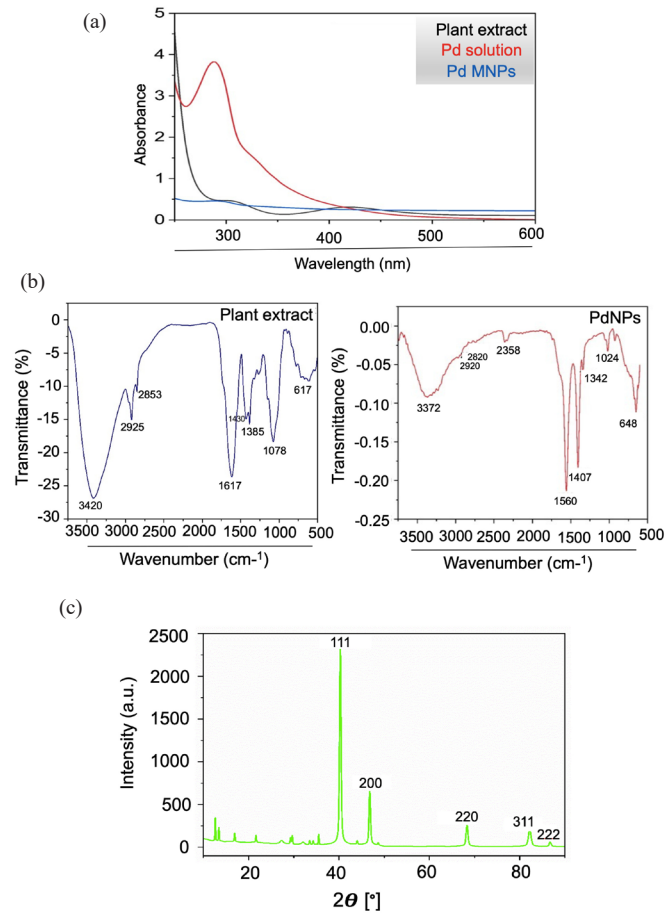

Fig. 2. (a) UV Visible spectrum of Plant extract, Pd^{2+} solution, and PdNPs. (b) FT-IR spectra of plant extract and PdNPs. (c) Powder XRD pattern of PdNPs. UV-Vis spectrum: Ultraviolet-Visible spectrum, PdNPs: Palladium nanoparticles, FT-IR: Fourier transform infrared spectroscopy, XRD: X-ray diffraction.

crystallographic planes of metallic palladium (Pd0) nanoparticles' fcc crystalline structure (JCPDS No: 89−4897) (111), (200), (220), (311), and (222) (Sarmah *et al.*, 2019; Wang *et al.*, 2015). In the determination of the average nanocrystalline size, the Debye–Scherrer method was employed (Al-Fakeh *et al.*, 2021). The formula $D = \lambda k/\beta\cos\theta$ was utilized, where D represents the crystal size, k is a constant with a value of 1, λ represents the X-ray wavelength (0.1541 nm), β is the full width at half maximum and θ corresponds to the diffraction angle related to the lattice plane (111). Application of the Debye–Scherrer equation revealed an average crystallite size of 5.58 nm.

3.4. FESEM and EDS analysis of PdNPs

Scanning electron microscopy (SEM) is a helpful technique utilized in materials science and numerous other fields to achieve high-resolution images of surfaces at the nanoscale. FESEM (Field Emission Scanning Electron Microscopy) is further enhanced with energy-dispersive X-ray spectroscopy (EDS) detectors, allowing for elemental analysis of the sample. According to the SEM images displayed in Fig. 3(a), it was observed that the PdNPs were almost spherical, even at higher resolutions. Additionally, these particles were evenly distributed on the surface with minimal clustering or agglomeration. The EDS spectrum detected unique signals based on the analysis of the elemental composition of PdNPs synthesized using *P. amboinicus* leaves extract. In Fig. 3(b), the absorption peaks ranging from 0.277 to 2.83 keV were attributed to forming PdNPs in the EDS spectra of PdNPs. In the EDX analysis, a strong signal for Pd was identified at 2.8 keV with a 57.92 weight percentage, indicating palladium PdNPs in the sample. In contrast, signals for C, O, N, and S were also present at 0.27, 0.52, 0.39, and 2.30 keV with 16.17, 16.60, 2.61, and 8.70 weight percentages, respectively, which is likely due to the plant leaf extract and conductive coating.

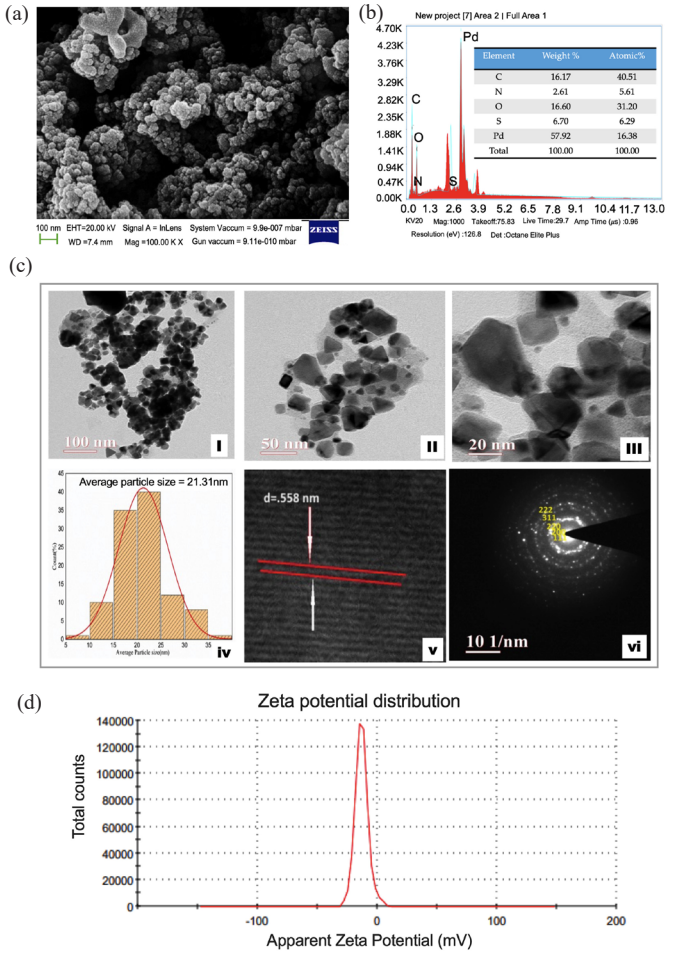

Fig. 3. (a) FESEM image and (b) EDX spectra of biosynthesized PdNPs. TEM image of PdNPs at 100 nm (c) HRTEM images of PdNPs at different magnifications (i) 50 nm and 20 nm magnification (ii-iii). Particle size distribution curve (iv). d-spacing of PdNPs (v). SAED pattern (vi). (d) Zeta potential of synthesized PdNPs. FESEM: Field emission scanning electron microscopy, EDX: Energy dispersive X-ray spectroscopy, TEM: Transmission electron microscopy, HRTEM: High-resolution transmission electron microscopy, SAED: Selected area electron diffraction, PdNP: Palladium nanoparticles.

3.5. TEM – HRTEM – SAED analysis

The particle size and structure of bio-inspired PdNPs were assessed by transmission electron microscopy (TEM), and the crystallinity was evaluated via selected area electron diffraction (SAED) pattern. According to the TEM – HRTEM images of PdNPs, they are triangular and rectangular shaped with particle sizes ranging from 5 to 40 nm displayed in Fig. 3c(I-III). The TEM image analyzed using ImageJ software revealed that the PdNPs have an average particle size of around 21.31 nm (Fig. 3c(iv)). Additionally, the lattice space was determined through HR-TEM, showing a d-space value of approximately 0.558 nm, as illustrated in Fig. 3c(v). The crystalline structure of plant-mediated PdNPs was established using the SAED pattern. Circular dots in the SAED pattern indicated the interplanar distances corresponding to the fcc crystalline structure of the PdNPs, including planes 111, 200, 220, and 311, confirming their crystalline nature (Fig. 3c(vi)). The PdNP sample's selected-area electron diffraction analysis displays clear concentric circles with bright intermittent spots, confirming the outstanding crystalline purity of the PdNPs. The diffraction patterns are categorized according to the PdNP crystallinity and are in line with JCPDS card No. 89-4897. The diffracted rings correspond to the crystallographic planes (111), (200), (220), (311), and (222) of the fcc PdNPs, and the results align with the XRD lattice plane of the PdNPs.

3.6. Zeta potential analysis

Zeta potential is paramount in colloidal systems as it measures the electrical charge at the interface between a particle surface and a liquid. It determines the stability and behavior of the system, making it vital in industrial and medical applications. The stability of PdNPs synthesized by the green method was determined by zeta potential parameters. Fig. 3(d) shows the zeta potential value for PdNPs is -12.9 mV. The zeta potential value of PdNPs suspension revealed even distribution and assessed its potential stability of particles (Aarzoo *et al.*, 2021; Al-Fakeh *et al.*, 2021). The synthesized PdNPs surfaces have a negative charge (-12.9 mV) and stable particle suspensions generally have a zeta potential range of +30 to -30 mV, as per published research (Han *et al.*, 2019).

3.7. Antibacterial assay

The synthesized PdNPs were assessed for their antibacterial efficiency against gram-positive and -negative bacteria. The results, as illustrated in Fig. 4(a), revealed that PdNPs have higher effectiveness than the plant extract and palladium chloride. Increase in the conc. of plant extract, Pd salt and PdNPs increased the zones of inhibition (Fig. 4b). The highest antibacterial effect with inhibition zone 14 ± 0.3 mm was observed against *Escherichia coli* with a minimum inhibitory concentration (MIC) of 5µg/mL. In contrast, the lower inhibition zone were observed against *B. subtilis, S. aureus* **and** *P. aeruginosa* with an MIC around 5 ± 0.3, 5± 0.6 and 5 ± 0.3 µg/mL with inhibition zone 11 ± 0.6, 11 ± 0.6 and 11 ± 0.4 mm respectively (Table 1). These findings suggest that PdNPs have a potent antibacterial effect, attributed to their ability to inhibit a broad range of bacterial strains (Gangwar *et al.*, 2023b; Jayakumar *et al.*, 2023; Sadalage and Pawar, 2023).

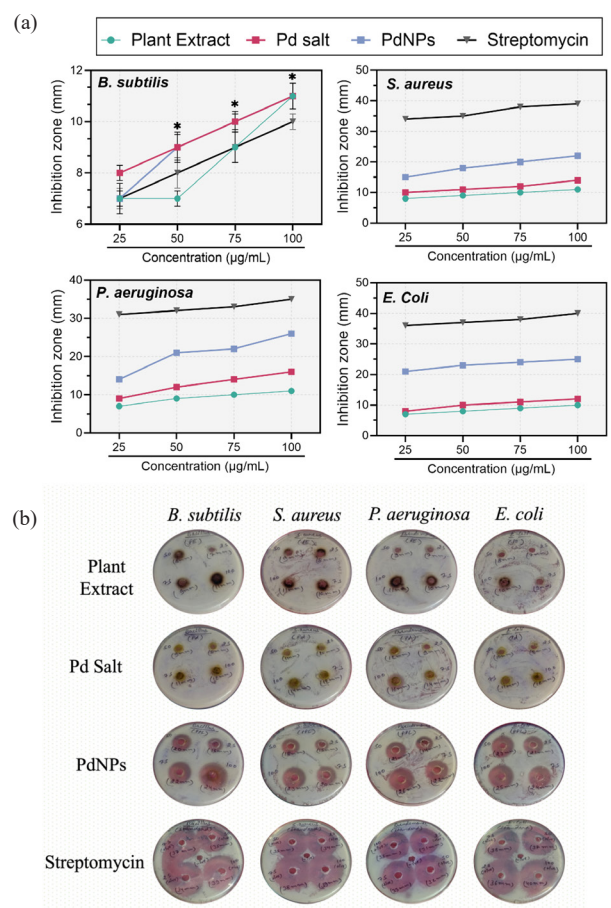

Fig. 4. Antimicrobial susceptibility of plant extracts, palladium chloride and PdNPs and streptomycin by disk diffusion method. (a) Antibacterial activity of plant extract, palladium chloride, PdNPs and streptomycin, (b) Zones of inhibition of plant extract, palladium chloride, PdNPs and streptomycin against the pathogenic strains *Bacillus subtilis, Staphylococcus aureus, Pseudomonas aeruginosa and Escherichia coli.* Results are shown as means ± S.D for triplicate with error bars indicating statistical significance at $p < 0.05$. PdNPs: Palladium nanoparticles, S.D.: Standard deviation.

Table 1.
Comparison of MIC and IZ for Plant extract, Pd salt and PdNPs.

Bacteria strains	Minimum inhibitory concentration (MIC) with inhibition zone (IZ)					
	Plant extract		Pd salt		PdNPs	
	MIC (µg/mL)	IZ (mm)	MIC (µg/mL)	IZ (mm)	MIC (µg/mL)	IZ (mm)
B. subtilis	25 ± 0.3	7 ± 0.4	18 ± 0.3	7 ± 0.5	5 ± 0.3	11 ± 0.6
S. aureus	18 ± 0.4	7 ± 0.6	15 ± 0.6	7 ± 0.4	5 ± 0.6	11 ± 0.6
P. areuginosa	25 ± 0.4	7 ± 0.4	15 ± 0.4	7 ± 0.3	5 ± 0.3	11 ± 0.4
E. coli	20 ± 0.6	7 ± 0.3	20 ± 0.3	7 ± 0.3	5 ± 0.6	14 ± 0.3

Pd salt: Palladium salt, PdNPs: Palladium nanoparticles

Once inside, Pd^{2+} ions bind to phosphorus and sulfur in proteins, or nucleic acid can ultimately destroy bacterial function (Skłodowski *et al.*, 2023; Tahir *et al.*, 2016).

3.8. Antioxidant assay

The *in vitro* antioxidant efficency of $PdCl_2$, *P. amboinicus* leaves extract, and PdNPs was estimated via a DPPH assay. The samples were measured for their absorbance against the DPPH radical at 517 nm using a UV−vis spectrophotometer. The findings demonstrated that the samples' capacity to scavenge DPPH radicals increased in a dose-responsive manner (Fig. 5a). Both the precursor salt $PdCl_2$ and *P. amboinicus* leaves exhibited the highest anti-DPPH scavenging activities at 1000 µg/mL, with values of 52.35 ± 0.08 and 50.50 ± 0.53, respectively. Meanwhile, DPPH radical scavenging percentages of PdNPs and ascorbic acid at 1000 µg/mL were 71.41 ± 0.94and 95.27 ± 0.88, respectively. The IC_{50}values of $PdCl_2$, *P. amboinicus* leave extract, and PdNPs were 773.81, 910.72, and 425.26 µg/mL, respectively (Fig. 5a). However, the IC_{50} values of precursor salt were much higher than those of the PdNPs and the positive control. The DPPH analysis indicates that the *P. amboinicus* leaves extract has less DPPH scavenging potency than PdNPs and ascorbic acid. Previous research has shown that PdNPs exhibit excellent antioxidant activity compared to precursor salts due to free charge transfer from the containing PdNPs to the DPPH radical (Gangwar *et al.*, 2023a; Tiri *et al.*, 2024).

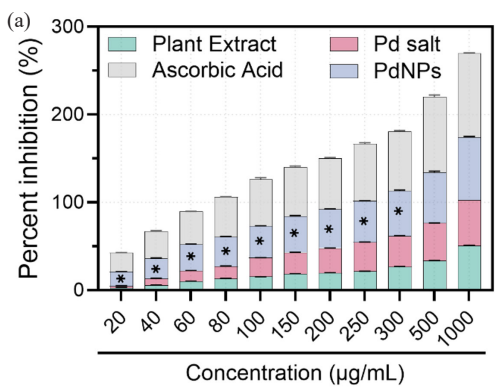

Concentration (µg/mL)	% scavenging activity (mean ± SD) against DPPH radical			
	Pd salt	Plant extract	PdNPs	Ascorbic acid
20	2.07 ± 0.63	2.44 ± 0.63	16.49 ± 0.23	21.67 ± 0.08
40	7.66 ± 0.31	5.54 ± 0.33	23.20 ± 0.37	30.97 ± 0.43
60	12.07 ± 0.28	10.07 ± 0.25	30.21 ± 0.27	37.32 ± 0.23
80	14.26 ± 0.26	12.98 ± 0.42	33.75 ± 0.28	45.13 ± 0.53
100	21.78 ± 0.16	15.25 ± 0.23	36.23 ± 0.11	53.02 ± 1.76
150	24.26 ± 0.36	18.71 ± 0.27	41.38 ± 0.69	56.05 ± 0.99
200	28.17 ± 0.23	19.70 ± 0.18	44.40 ± 0.39	57.91 ± 1.04
250	33.20 ± 0.17	21.41 ± 0.14	46.96 ± 0.28	64.99 ± 1.40
300	35.28 ± 0.21	26.56 ± 0.26	51.30 ± 1.04	67.40 ± 1.42
500	43.05 ± 0.11	33.53 ± 0.27	57.91 ± 1.01	85.93 ± 1.90
1000	52.35 ±0.08	50.50 ± 0.53	71.41 ± 0.94	95.27 ± 0.88
IC_{50} (µg/mL)	773.81	910.72	425.26	158.26

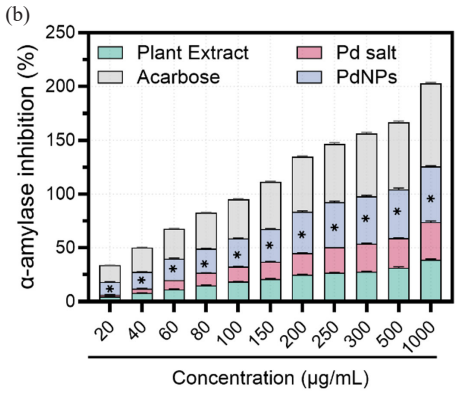

Concentration (µg/mL)	% alpha-amylase inhibition (mean ± SD)			
	Pd salt	Plant extract	PdNPs	Acarbose
20	1.65 ± 0.25	4.83 ± 0.21	12.05 ± 0.14	15.31 ± 0.15
40	4.17 ± 0.20	8.09 ± 0.17	15.35 ± 0.21	22.71 ± 0.33
60	8.63 ± 0.06	11.52 ± 0.25	19.98 ± 0.62	27.82 ± 0.15
80	11.52 ± 0.24	15.19 ± 0.33	22.5 ± 0.42	33.69 ± 0.16
100	13.75 ± 0.39	18.62 ± 0.3	26.47 ± 0.32	36.33 ± 0.59
150	16.1 ± 0.22	21.18 ± 0.33	30.3 ± 0.41	43.81 ± 0.67
200	19.9 ± 0.3	25.31 ± 0.15	38.4 ± 0.83	51.2 ± 0.63
250	23.78 ± 0.06	26.68 ± 0.43	42.36 ± 0.7	53.76 ± 1.22
300	26.0 2 ± 0.61	27.87 ± 0.38	43.98 ± 0.97	58.67 ± 0.9
500	27.62 ± 0.25	31.54 ± 0.93	45.18 ± 1.24	62.27 ± 1.24
1000	34.89 ± 0.86	39.11 ± 0.73	51.78 ± 0.6	77.25 ± 0.79
IC_{50} (µg/mL)	1009.53	817.31	547.75	272.59

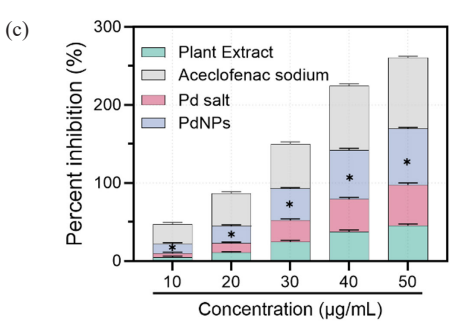

Concentration (µg/mL)	% Bovine serum albumin inhibition (mean ± SD)			
	Pd salt	Plant extract	PdNPs	Aceclofenac sodium
10	4.85 ±1.02	5.32 ± 1.63	11.60 ± 1.58	25.49 ± 2.23
20	10.70 ±1.09	12.53 ± 1.40	21.85 ± 1.42	41.54 ± 2.27
30	24.90 ±1.50	27.51 ± 1.59	40.53 ± 1.06	56.70 ± 2.79
40	37.60 ±2.13	41.84 ± 2.10	62.32 ± 2.61	82.93 ± 2.66
50	45.71 ±2.34	51.89 ± 1.99	72.00 ± 1.76	90.90 ± 1.91
IC_{50} (µg/mL)	53.24	48.12	35.17	24.47

Fig. 5. (a) DPPH radical scavenging activities of Pd salt, plant extract, PdNPs and ascorbic acid, (b) Anti-diabetic assay of Pd salt, plant extract, PdNPs and acarbose, (c) Anti-inflammatory activity of Pd salt, plant extract, PdNPs and aceclofenac sodium by analysing the percentage bovine serum albumin inhibition of respective groups. Results are shown as means ± S.D for triplicate with error bars trough one-way analysis of variance (ANOVA) and Tukey multiple comparison test indicating statistical significance at $^*p < 0.05$. DPPH: 2,2-Diphenyl-1-picrylhydrazyl, Pd salt: Palladium salt, PdNPs: Palladium nanoparticles, BSA: Bovine serum albumin, S.D.: Standard deviation, IC_{50}: Half-maximal inhibitory concentration.

Table 2.
Comparison of metal and metal oxide nanoparticles' DPPH scavenging capabilities.

Nano-particles	Average size (nm)	Concentration	DPPH scavenging (%)	References
PdNPs	21.31	1000 µg/mL	71.41	Present study
AgNPs	9.1	250 µg/mL	80.00	Gur *et al.*, 2025
AuNPs	5-23	300 µg/mL	57.70	Hosny *et al.*, 2021
PtNPs	1-3	50 µg/mL	72.00	Eltaweil *et al.*, 2022
PdNPs	7.44	500 mg/L	79.60	Gulbagca *et al.*, 2021
CuO-NPs	35.8-49.2	500 µg/mL	29.30	Das *et al.*, 2020
ZnO-NPs	8-12	100 µg/mL	81.92	Ghareib *et al.*, 2019

PdNPs: Palladium nanoparticles, AgNPs: Silver nanoparticles, AuNPs: Gold nanoparticles, PtNPs: Platinum nanoparticles, CuO-NPs: Copper oxide nanoparticles, ZnO-NPs: Zinc oxide nanoparticles, DPPH: 2,2-Diphenyl-1-picrylhydrazyl.

A study of phytochemical-synthesized AgNPs (9.1 nm) showed DPPH scavenging activity of 80% at 250 µg/mL (Gur *et al.*, 2025). Another study on biosynthesized AuNPs (5-23 nm) indicated 57.7% scavenging at 300 µg/mL (Hosny *et al.*, 2021). Research on plant-mediated PtNPs (1-3 nm) and PdNPs (7.4 nm) found scavenging activities of 72.0% at 50 µg/mL and 79.6% at 500 mg/mL, respectively (Eltaweil *et al.*, 2022; Gulbagca *et al.*, 2021). Additionally, studies on CuO-NPs (35.8-49.2 nm) and ZnO-NPs (8-12 nm) revealed scavenging activities of 29.30% at 500 µg/mL and 81.92% at 100 µg/mL (Das *et al.*, 2020; Ghareib *et al.*, 2019). The findings reveal that both particle size and concentration play a notable role in modifying antioxidant activity. To provide a more robust evaluation of our results, we performed a comparative analysis alongside the findings of other metal and metal oxide nanoparticles, as outlined in Table 2. Therefore, the biosynthesized PdNPs from the *P. amboinicus* leaves extract could be a promising antioxidant drug for oxidative stress-related ailments.

3.9. Anti-diabetic assay

α-amylase is an enzyme that has a critical function in converting complex carbohydrates into simpler sugars. Inhibiting α-amylase can be beneficial in managing blood sugar levels in individuals with diabetes, or as a potential strategy for weight control. In this study, biosynthesized PdNPs were evaluated for their anti-diabetic activity by measuring the inhibition of α-amylase. When this enzyme is inhibited, the absorption rate of glucose can be reduced. Acarbose was used as a control to serve as a reference point, and the results showed a 77.00% inhibition at the conc. of 1000 µg/mL. The biosynthesized PdNPs showed a more substantial inhibition of α-amylase than the $PdCl_2$ and plant extract. Fig. 5(b) provides the percentage inhibition and IC_{50} values for the PdNPs, plant extract, and control. The results indicated that biosynthesized PdNPs exhibited higher inhibition of alpha-amylase than the *P. amboinicus* leaves extract and the palladium salt. A maximum inhibition (51.78%) of alpha-amylase was observed at 1000 µg/mL by biosynthesized PdNPs. Fig. 5(b) shows a graphical representation of alpha-amylase inhibition.

A comparison of biosynthesized PdNPs with other metal and metal oxide nanoparticles, including AgNPs (Rehman *et al.*, 2023), AuNPs (Rokkarukala *et al.*, 2023), CuO-NPs (Ameena *et al.*, 2022), and ZnO-NPs (Rehman *et al.*, 2023) has been illustrated in Table 3, highlighting the moderate anti-diabetic properties of biosynthesized PdNPs.

3.10. Anti-inflammatory assay

The results of the anti-inflammatory assay suggest that the biosynthesized PdNPs were more effective in inhibiting bovine serum albumin than the *P. amboinicus* leaves extract and the palladium salt (Fig. 5c). The analysis showed a significant relationship between PdNPs and protein denaturation (72.00% inhibition at 50 µg/mL and the *P. amboinicus* leaves extract (51.89% inhibition). The Pd salt and *P. amboinicus* leaves extract showed inhibition ranging from 4.85% to 45.71% and 5.32 % to 51.89 % respectively and biosynthesized PdNPs showed anti-inflammatory activity ranging from 11.60% to 72.00% at concentration 10-50 µg/mL (Fig. 5c). These findings align with other studies using PdNPs synthesized from diverse medicinal plants (Bi and Srivastava, 2024; Sandhya *et al.*, 2024).

Table 3.
Comparison of the anti-diabetic efficiencies of metal nanoparticles and metal oxide nanoparticles.

Nano-particles	Average size (nm)	Concentration	Inhibition of alpha-amylase (%)	References
PdNPs	21.31	1000 µg/mL	51.78	Present study
AgNPs	34.43	100 µg/mL	75.00	Rehman *et al.*, 2023
AuNPs	5-50	100 µg/mL	68.00	Rokkarukala *et al.*, 2023
CuO-NPs	63.46	100 µg/mL	64.50	Ameena *et al.*, 2022
ZnO-NPs	16-28	100 µg/mL	71.90	Rehman *et al.*, 2023

PdNPs: Palladium nanoparticles, AgNPs: Silver nanoparticles, AuNPs: Gold nanoparticles, CuO-NPs: Copper oxide nanoparticles, ZnO-NPs: Zinc oxide nanoparticles

Table 4.
Comparison of the *anti-inflammatory* activity of metal nanoparticles and metal oxide nanoparticles.

Nano-particles	Average size (nm)	Concentration	Protein denaturation (%)	References
PdNPs	21.31	50 µg/Ml	72.00	Present study
AgNPs	15.96	20 mg/kg	57.08	Sharifi-Rad *et al.*, 2020
AuNPs	34.2	500 µg/mL	82.00	Khuda *et al.*, 2021
CuO-NPs	6.89	500 µg/mL	75.16	Manasa *et al.*, 2021
ZnO-NPs	70.37	50 µg/mL	77.89	Nandhini *et al.*, 2025

PdNPs: Palladium nanoparticles, AgNPs: Silver nanoparticles, AuNPs: Gold nanoparticles, CuO-NPs: Copper oxide nanoparticles, ZnO-NPs: Zinc oxide nanoparticles.

A study on phytochemicals used to synthesize AgNPs (34.2 nm) showed an *anti-inflammatory* activity of 82% at 500 µg/mL (Sharifi-Rad *et al.*, 2020). Biosynthesized AuNPs (15.96 nm) had an *anti-inflammatory activity* of 57.7% at 20 mg/kg (Khuda *et al.*, 2021). CuO-NPs (6.89 nm) and ZnO-NPs (70.37 nm) exhibited *anti-inflammatory* activities of 75.16% at 500 µg/mL and 77.89% at 50 µg/mL (Manasa *et al.*, 2021; Nandhini *et al.*, 2025). A comparison between biosynthesized PdNPs and other nanoparticles (AgNPs, AuNPs, CuO-NPs and ZnO-NPs) to suggest the higher protein denaturation efficacy of biosynthesized PdNPs has been presented in Table 4. The eco-friendly synthesis of PdNPs demonstrated excellent anti-inflammatory properties without any negative impacts typically associated with chemically synthesized medications.

3.11. Wound healing efficacy

In addition to its antibacterial properties, PdNPs also exhibit anti-inflammatory activity, which collectively contributes to their remarkable wound-healing efficacy. In this study, all the animals treated with PdNPs showed a sizable increase in the percentage of healed wounds in comparison with the control groups during the 18-day experiment using the excision wound model. Application of the PdNPs for 10 days led to 74.76% wound being healed compared to 55.56 % of negative control animals and 80.77 % of the positive control group *i.e.* nitrofurazone (0.2%w/w) ointment treated. The area of the wound expressed in mm^2 reduced significantly faster in the PdNPs treated and positive control group compared to control group. It has taken 14 days to heal completely using the PdNPs compared to 18 days in the negative control group and 14 days in the positive control group. Photographs taken on the 1, 6, 12, and 18th day also reflect the same (Fig. 6a). The efficiency of PdNPs in facilitating wound healing is reflected in both the percentage of wound contraction(mm^2) and the faster reduction

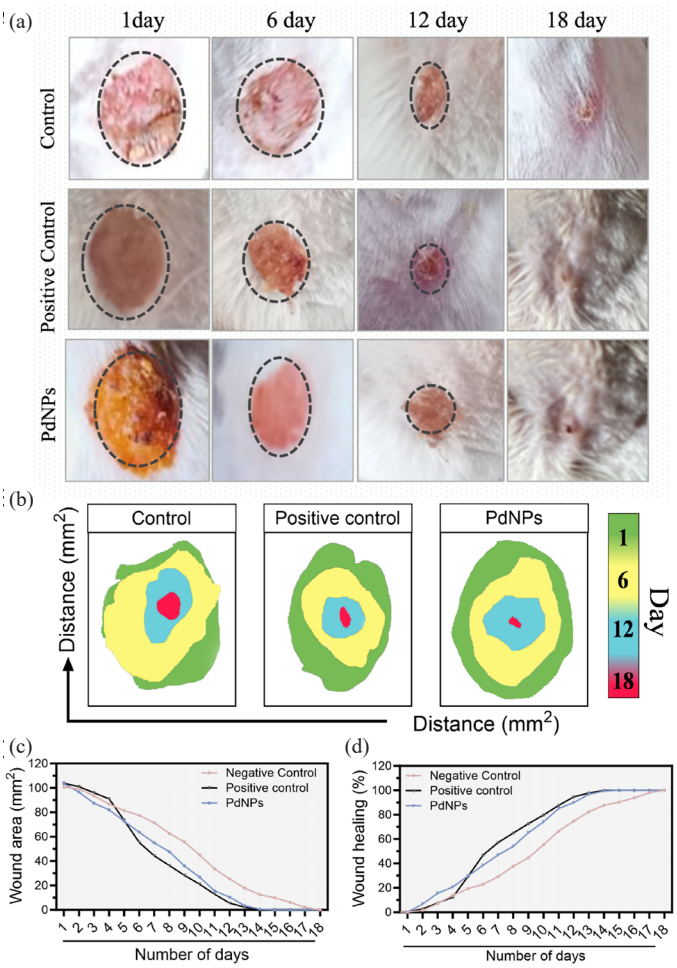

Fig. 6. *In vivo* wound healing efficacy study in mice. (a) Representative photographs capturing the wound healing process at specific timepoints (days 0, 6, 12, and 18) in different treatment groups: control (untreated), PdNPs-treated, and positive control (nitrofurazone 0.2% w/w ointment). (b) Simulation analysis photographs of wound healing with respective treatments, (c) Effect of treatments on wound contraction (mm^2) over time across the treatment groups. (d) A comparison of the Percentage of wound healed between the PdNPs, positive control compared to control with $p<0.05$ statistically significant difference in comparison with untreated group. PdNPs: Palladium nanoparticles.

in wound area observed in this study compared to control have been depicted in Fig. (6a-d), respectively (Arumugam *et al.*, 2024; Hamid *et al.*, 2024; He *et al.*, 2022; Yin *et al.*, 2023).

Nanoparticles play a critical role in wound healing by moderating biological mechanisms like cellular migration, proliferation, angiogenesis, and antimicrobial defense. PdNPs exhibit promising wound-healing potential due to their ability to generate ROS in controlled amounts (Mubarak-Ali *et al.*, 2023), which act as signaling molecules to promote angiogenesis and fibroblast migration (Liu *et al.*, 2024). Additionally, PdNPs modulate oxidative stress by balancing ROS levels, creating an optimal environment for tissue repair. They can also initiate key signaling mechanisms such as PI3K/AKT and MAPK (Kumar and Sood, 2020), which regulate keratinocyte proliferation and migration, as well as upregulate vascular endothelial growth factor (VEGF) to enhance angiogenesis and collagen synthesis (Khosravi and Khamari, 2019). These mechanisms make PdNPs a valuable candidate for wound-healing applications, particularly when incorporated into advanced nano scaffolds or drug delivery systems.

Compared to other nanoparticles, PdNPs are uniquely advantageous in their recyclability and catalytic properties, which can be leveraged for sustained therapeutic effects (Liu and Zheng, 2017). AgNPs excel in antimicrobial activity, disrupting microbial membranes and generating ROS (Rai *et al.*, 2009), while AuNPs are highly biocompatible and effective in promoting keratinocyte growth and angiogenesis at low concentrations (Dykman and Khlebtsov, 2012). Cerium oxide nanoparticles (CeO_2 NPs) function as redox modulators, scavenging excessive ROS and activating angiogenic pathways such as hypoxia-inducible factor-1α (HIF-1α) (Sreejith *et al.*, 2016). Although PdNPs may require functionalization to enhance their antimicrobial efficacy, they provide a versatile and cost-effective alternative for wound-healing applications due to their superior catalytic efficiency and balanced ROS modulation (Zhang and Liu, 2019).

A comparison of wound healing activity of biosynthesized PdNPs alongside various other types of nanoparticles, including AgNPs (Chinnasamy *et al.*, 2021), AuNPs (Soliman *et al.*, 2022) and ZnO-NPs (Shoukani *et al.*, 2024), has been provided in Table 5. This comparison underscores the significant wound healing properties demonstrated by the biosynthesized PdNPs, showcasing their potential use in wound healing dressing.

Conventional nanoparticle synthesis methods often use toxic solvents, require high energy input, and generate hazardous byproducts, endangering the environment and human health. Eco-friendly synthesis methods using plant extracts or green chemistry present a promising alternative to reduce environmental costs and have the prospective to lead to more economical and ecologically sustainable production in the long run. MNPs, including silver, gold, and zinc oxide, present significant safety concerns primarily because of their small size and distinct physicochemical features. These nanoparticles can easily penetrate biological barriers such as cell membranes, leading to potential cytotoxic effects. This cytotoxicity can stem from various mechanisms, including ROS production, which contribute to oxidative stress within cells. Oxidative stress can disrupt cellular homeostasis, leading to inflammation as the immune system responds to the perceived threat of these foreign particles.

In Table 6, a comparison is made between the safety, sustainability, and cost-effectiveness of biosynthesized PdNPs and various other types of nanoparticles, including AgNPs (Bharathi *et al.*, 2024), AuNPs (Khan *et al.*, 2024), PtNPs (Shabani *et al.*, 2023), CuO-NPs (Khairy *et al.*, 2024), and ZnO-NPs (Alnehia *et al.*, 2022). This comparison highlights the biosynthesis method for producing PdNPs using aqueous leaf extract from *P. amboinicus*, which is not only sustainable and more economical but also uses less time and energy compared to the synthesis of other nanoparticles. Oxidative stress may result from an excess of ROS production, impairing the cells' ability to maintain normal physiological redox-regulated functions. This disruption to cell function and development can result in oxidative modifications of proteins, the generation of protein radicals, DNA strand breaks, and nucleic acid modifications, ultimately leading to cell death and genotoxic effects. Additionally, in contrast to other metal and metal oxide nanoparticles, biosynthesized PdNPs demonstrate lower toxicity toward *E. coli* bacterial cells. The toxicity is affected by the type of nanomaterial, its shape, size, surface charge, and the specific bacterial strain involved, as shown in Table 6.

Table 5.
A comparison of wound healing activity of biosynthesized PdNPs alongside various other types of nanoparticles.

Nano-particles	Types of wound healing agents	Dosages/ con-centration	Wound contraction (%)	Exposure to wound area	References
PdNPs	Ointment	1% w/w	74.76	10 days	Present study
AgNPs	Hydrogel	30% w/v	60.42	10 days	Chinnasamy *et al.*, 2021
AuNPs	Ointment	30 μg/kg	80.00	14 days	Soliman *et al.*, 2022
PEG coated ZnO-NPs	Spray	10 mg /500 μL	89.00	10 days	Shoukani *et al.*, 2024

PdNPs: Palladium nanoparticles, AgNPs: Silver nanoparticlesm, AuNPs: Gold nanoparticlesm, ZnO-NPs: Zinc oxide nanoparticles, w/w: Weight/Weight, w/v: Weight/Volume, PEG: Polyethylene glycol.

Table 6.
A comparison of sustainability cost-effectiveness and safety for metal and metal oxide nanoparticles.

Nanoparticles	Sustainability	Cost-effectiveness	Safety				References
	Synthesis method/ Biological entity	Reaction conditions	(ROS-related toxicity)				
			Average size (nm)	Shape of particles	Dosages/ Conc.	Inhibition zone (mm) for *E. coli*	
PdNPs	Green Synthesis / *Plectranthus amboinicus* leaf extract	80°C, 30 min.	21.31	Triangular and rectangular	100 µg/mL	14.03	Present study
AgNPs	Green Synthesis / kiwi fruit peel extract	27°C, 3 h	10-70	Cubic	50 µg/mL	16.00	Bharathi *et al.*, 2024
AuNPs	Green Synthesis / *Callistemon viminalis* extract	80°C, 24 h	100	Circular	0.2 mg/mL	11.50	Khan *et al.*, 2024
PtNPs	Green Synthesis / *Penicillium pinophilum* cell-free filtrate	25°C, 24 h	2–30	Spherical	100 µg/mL	19.20	Shabani *et al.*, 2023
CuO-NPs	Green Synthesis / *Azadirachta indica* leaf extract	30°C, 24 h	30.9	Semispherical	100 µg/mL	19.00	Khairy *et al.*, 2024
ZnO-NPs	Green Synthesis / pomegranate peel aqueous extract	25°C, 90 min.	30.34	Spherical	100 mg/mL	27.00	Alnehia *et al.*, 2022

PdNPs: Palladium nanoparticles, AgNPs: Silver nanoparticles, AuNPs: Gold nanoparticles, PtNPs: Platinum nanoparticles, CuO-NPs: Copper oxide nanoparticles, ZnO-NPs: Zinc oxide nanoparticles, ROS: Reactive oxygen species.

4. Conclusion

In conclusion, this study showcases the successful green and bio-inspired synthesis of PdNPs using biogenic reduction through aqueous leaf extract of *P. amboinicus*. Numerous characterization methods were utilized, including UV-Vis spectroscopy, FTIR, FESEM, EDS, high-resolution TEM, XRD, and zeta potential analysis. The synthesized PdNPs demonstrated the structural and morphological properties of the PdNPs, while biological assays demonstrated their multifunctional therapeutic potential, including significant antibacterial activity. Notably, enhanced wound healing efficacy in laboratory mice was observed within a period of 14 days emphasizing their suitability for diverse biomedical applications. Moving forward, future research may focus on conducting in-depth *in vivo* studies to further validate the mechanistic activities of PdNPs and their potential in drug delivery. This study offers an excellent starting point for scientists interested in the field of nanobiotechnology and nanomedicine, providing insight into nanocarrier systems and drug delivery metabolism.

The future prospects of biosynthesized PdNPs for wound healing are highly promising due to their ability to modulate oxidative stress, enhance angiogenesis, and promote cellular proliferation through ROS-mediated signaling pathways. Advancements in functionalization and integration with biomaterials could further optimize their therapeutic efficacy, biocompatibility, and targeted delivery, paving the way for innovative wound-care solutions.

CRediT authorship contribution statement

Ashwini Singhal: Investigation, Formal analysis, Writing – original draft, Visualization. **Gyan Prakash Meghwal:** Investigation, Formal analysis. **Apurva Jaiswal:** Investigation, Formal analysis. **Neha Kaushik:** Investigation, Formal analysis. **Anita Kumari:** Investigation, Formal analysis. **Nighat Fahmi:** Investigation, Validation, Formal analysis. **Rizwan Wahab:** Writing – review, editing & Funding acquisition. **Dev Dutt Patel:** Investigation, Validation, Formal analysis. **Abdulaziz A. Al-Khedhairy:** Writing – review, editing & Funding acquisition. **Priyadarshi Meena:** Supervision, Resources, Writing – review & editing. **Nagendra Kumar Kaushik:** Supervision, Resources, Writing – review, editing & Funding acquisition. **Ramhari Meena:** Conceptualization, Methodology, Supervision, Resources, Writing – review & editing, Funding acquisition. All authors have read and agreed to the published version of the manuscript.

Declaration of competing interest

The authors declare that they have no known competing financial interests or personal relationships that could have appeared to influence the work reported in this paper.

Declaration of Generative AI and AI-assisted technologies in the writing process

The authors confirm that there was no use of artificial intelligence (AI)-assisted technology for assisting in the writing or editing of the manuscript and no images were manipulated using AI.

Acknowledgements

The authors would like to thank Dr. Chitra Jain, Biomitra Life Sciences Pvt. Ltd for their generous help during in vitro antibacterial, antioxidant, anti-diabetic, and anti-inflammatory experiments. Additionally, we would like to extend our thanks to the CSIR-University Grant Commission for providing financial assistance to one of our authors, Ashwini Singhal (Grant No. 274/(CSIR-UGC NET 2018), New Delhi, India).

Funding

This research was funded by the National Research Foundation (NRF) of Korea, (2021R1A6A1A03038785) and by Kwangwoon University in 2024. The authors are also grateful to the Deanship of Scientific Research , King Saud University for funding through Vice Deanship of Scientific Research Chairs: Chair for DNA Research.

References

Aarzoo, N., Naqvi, S., Agarwal, N.B., Singh, M.P., Samim, M., 2021. Bio-engineered palladium nanoparticles: Model for risk assessment study of automotive particulate pollution on macrophage cell lines. RSC Adv. 11, 1850-1861. https://doi.org/10.1039/d0ra09336j

Aarzoo, N., Nidhi, N., Samim, M., 2022. Palladium nanoparticles as emerging pollutants from motor vehicles: An in-depth review on distribution, uptake and toxicological effects in occupational and living environment. Sci. Total Environ. 823, 153787. https://doi.org/10.1016/j.scitotenv.2022.153787

Al-Fakeh, M.S., Osman, S.O.M., Gassoumi, M., Rabhi, M., Omer, M., 2021. Characterization, antimicrobial and anticancer properties of palladium nanoparticles biosynthesized optimally using saudi propolis. Nanomaterials 11, 2666. https://doi.org/10.3390/nano11102666

Alinaghi, M., Mokarram, P., Ahmadi, M., Bozorg-Ghalati, F., 2024. Biosynthesis of palladium, platinum, and their bimetallic nanoparticles using rosemary and ginseng herbal plants: Evaluation of anticancer activity. Sci. Rep. 14, 5798. https://doi.org/10.1038/s41598-024-56275-z

Alnehia, A., Al-Odayni, A.-B., Al-Sharabi, A., Al-Hammadi, A.H., Saeed, W.S., 2022. Pomegranate peel extract-mediated green synthesis of znO-NPs: Extract concentration-dependent structure, optical, and antibacterial activity. J. Chem. 2022, 1-11. https://doi.org/10.1155/2022/9647793

Ameena, S., Rajesh, N., Anjum, S.M., Khadri, H., Riazunnisa, K., Mohammed, A., Kari, Z.A., 2022. Antioxidant, antibacterial, and anti-diabetic activity of green synthesized copper nanoparticles of cocculus hirsutus (Menispermaceae). Appl. Biochem. Biotechnol. 194, 4424-4438. https://doi.org/10.1007/s12010-022-03899-4

Arsiya, F., Sayadi, M.H., Sobhani, S., 2017. Arsenic (III) Adsorption Using Palladium Nanoparticles from Aqueous Solution. J. Water Environ. Nanotechnol. J. Water Environ. Nanotechnol 2, 166–173. https://doi.org/10.22090/jwent.2017.03.004

Arteaga-Castrejón, A.A., Agarwal, V., Khandual, S., 2024. Microalgae as a potential natural source for the green synthesis of nanoparticles. Chem. Commun. (Camb). 60, 3874-3890. https://doi.org/10.1039/d3cc05767d

Arumugam, M., Murugesan, B., Chinnalagu, D., Balasekar, P., Cai, Y., Sivakumar, P.M., Rengasamy, G., Chinniah, K., Mahalingam, S., 2024. Electrospun silk fibroin and collagen composite nanofiber incorporated with palladium and platinum nanoparticles for wound dressing applications. J. Polym. Environ. 32, 2797-2817. https://doi.org/10.1007/s10924-024-03261-1

Arya, A., Tyagi, P.K., Bhatnagar, S., Bachheti, R.K., Bachheti, A., Ghorbanpour, M., 2024. Biosynthesis and assessment of antibacterial and antioxidant activities of silver nanoparticles utilizing cassia occidentalis l. seed. Sci. Rep. 14, 7243. https://doi.org/10.1038/s41598-024-57823-3

Atchaya, S., Meena Devi, J., 2024. Experimental investigation on structural, optical, electrical and magnetic properties of copper oxide nanoparticles. Proc. Natl. Acad. Sci., India, Sect. A Phys. Sci. 94, 153-160. https://doi.org/10.1007/s40010-023-00855-7

Augustus, A.R., Jana, S., Samsudeen, M.B., Nagaiah, H.P., Shunmugiah, K.P., 2024. In vitro and in vivo evaluation of the anti-infective potential of the essential oil extracted from the leaves of plectranthus amboinicus (lour.) spreng against klebsiella pneumoniae and elucidation of its mechanism of action through proteomics approach. J. Ethnopharmacol. 330, 118202. https://doi.org/10.1016/j.jep.2024.118202

Basavegowda, N., Mishra, K., Lee, Y.R., 2015. Ultrasonic-assisted green synthesis of palladium nanoparticles and their nanocatalytic application in multicomponent reaction. New J. Chem. 39, 972-977. https://doi.org/10.1039/c4nj01543f

Bharathi, D., Lee, J., Karthiga, P., Mythili, R., Devanesan, S., AlSalhi, M.S., 2024. Kiwi fruit peel biowaste mediated green synthesis of silver nanoparticles for enhanced dye degradation and antibacterial activity. Waste Biomass Valor. 15, 1859-1868. https://doi.org/10.1007/s12649-023-02328-9

Bi, S., Srivastava, R., 2024. Rosa damascena leaf extract mediated palladium nanoparticles and their anti-inflammatory and analgesic applications. Inorg. Chem. Commun. 162, 112122. https://doi.org/10.1016/j.inoche.2024.112122

Bokolia, M., Baliyan, D., Kumar, A., Das, R., Kumar, R., Singh, B., 2024. Biogenic synthesis of nanoparticles using microbes and plants: Mechanisms and multifaceted applications. Int. J. Environ. Anal. Chem., 1-29. https://doi.org/10.1080/03067319.2024.2305238

C, F.C., T, K., 2024. Advances in stabilization of metallic nanoparticle with biosurfactants- a review on current trends. Heliyon 10, e29773. https://doi.org/10.1016/j.heliyon.2024.e29773

Cai, J., Zhang, C., Khan, A., Wang, L., Li, W.D., 2018. Selective electroless metallization of micro- and nanopatterns via poly(dopamine) modification and palladium nanoparticle catalysis for flexible and stretchable electronic applications. ACS Appl. Mater. Interfaces 10, 28754-28763. https://doi.org/10.1021/acsami.8b07411

Chen, W.-D., Lin, Y.-H., Chang, C.-P., Sung, Y., Liu, Y.-M., Ger, M.-D., 2011. Fabrication of high-resolution conductive line via inkjet printing of nano-palladium catalyst onto PET substrate. Surf. Coat. Technol. 205, 4750-4756. https://doi.org/10.1016/j.surfcoat.2011.03.043

Chinnasamy, G., Chandrasekharan, S., Koh, T.W., Bhatnagar, S., 2021. Synthesis, characterization, antibacterial and wound healing efficacy of silver nanoparticles from azadirachta indica. Front. Microbiol. 12, 611560. https://doi.org/10.3389/fmicb.2021.611560

Das, P.E., Abu-Yousef, I.A., Majdalawieh, A.F., Narasimhan, S., Poltronieri, P., 2020. Green synthesis of encapsulated copper nanoparticles using a hydroalcoholic extract of moringa oleifera leaves and assessment of their antioxidant and antimicrobial activities. Molecules 25, 555. https://doi.org/10.3390/molecules25030555

Dauthal, P., Mukhopadhyay, M., 2013. Biosynthesis of palladium nanoparticles using delonix regia leaf extract and its catalytic activity for nitro-aromatics hydrogenation. Ind. Eng. Chem. Res. 52, 18131-18139. https://doi.org/10.1021/ie403410z

Dhumal, K., Dateer, R., Mali, A., 2024. Recent catalytic advancements in organic transformations using biogenically synthesized palladium nanoparticles. Catal. Lett. 154, 329-351. https://doi.org/10.1007/s10562-022-04258-y

Dykman, L., Khlebtsov, N., 2012. Gold nanoparticles in biomedical applications: Recent advances and perspectives. Chem. Soc. Rev. 41, 2256-2282. https://doi.org/10.1039/c1cs15166e

El-Khawaga, A.M., Zidan, A., El-Mageed, A.I.A.A., 2023. Preparation methods of different nanomaterials for various potential applications: A review. J. Mol. Struct. 1281, 135148. https://doi.org/10.1016/j.molstruc.2023.135148

Eltaweil, A.S., Fawzy, M., Hosny, M., Abd El-Monaem, E.M., Tamer, T.M., Omer, A.M., 2022. Green synthesis of platinum nanoparticles using atriplex halimus leaves for potential antimicrobial, antioxidant, and catalytic applications. Arab. J. Chem. 15, 103517. https://doi.org/10.1016/j.arabjc.2021.103517

Emam, H.E., 2022. Accessibility of green synthesized nanopalladium in water treatment. Results Eng. 15, 100500. https://doi.org/10.1016/j.rineng.2022.100500

Gangwar, C., Yaseen, B., Kumar, I., Nayak, R., Sarkar, J., Baker, A., Kumar, A., Ojha, H., Singh, N.K., Naik, R.M., 2023. Nano palladium/palladium oxide formulation using ricinus communis plant leaves for antioxidant and cytotoxic activities. Inorg. Chem. Commun. 149, 110417. https://doi.org/10.1016/j.inoche.2023.110417

Gangwar, C., Yaseen, B., Nayak, R., Baker, A., Bano, N., Singh, N.K., Naik, R.M., 2023. Madhuca longifolia leaves-mediated palladium nanoparticles synthesis via a sustainable approach to evaluate its biomedical application. Chem. Pap. 77, 3075-3091. https://doi.org/10.1007/s11696-023-02688-5

Gupta, D., Boora, A., Thakur, A., Gupta, T.K., 2023. Green and sustainable synthesis of nanomaterials: Recent advancements and limitations. Environ. Res. 231, 116316. https://doi.org/10.1016/j.envres.2023.116316

Gulbagca, F., Aygün, A.şenur, Gülcan, M., Ozdemir, S., Gonca, S., Şen, F., 2021. Green synthesis of palladium nanoparticles: Preparation, characterization, and investigation of antioxidant, antimicrobial, anticancer, and DNA cleavage activities. Appl. Organomet. Chem. 35. https://doi.org/10.1002/aoc.6272

Gupta, K., Gautre, P., Biharee, A., Singh, Y., Patil, U.K., Kumar, S., Thareja, S., 2024. Exploring the potential of essential oil from plectranthus amboinicus leaves against breast cancer: In vitro and in silico analysis. Med. Oncol. 41, 81. https://doi.org/10.1007/s12032-024-02325-5

Gur, T., Bekmezci, M., Meydan, I., Seckin, H., Sen, F., 2025. Characterisation, antibacterial and antioxidant effects of mountain tea (Sideritis l.) mediated silver nanoparticles in preventing DNA damage. Int. J. Environ. Sci. Technol. 22, 1567-1576. https://doi.org/10.1007/s13762-024-05746-x

Hamid, L.L., Hassan, M.H., Obaid, A.S., 2024. Allium sativum extract mediate the biosynthesis of palladium nanoparticles as potential nanodrug for combating multidrug-resistant bacteria and wound healing. Mater. Chem. Phys. 321, 129507. https://doi.org/10.1016/j.matchemphys.2024.129507

Han, Z., Dong, L., Zhang, J., Cui, T., Chen, S., Ma, G., Guo, X., Wang, L., 2019. Green synthesis of palladium nanoparticles using lentinan for catalytic activity and biological applications. RSC Adv. 9, 38265-38270. https://doi.org/10.1039/c9ra08051a

He, J., Wang, J., Gao, S., Cui, Y., Ji, X., Zhang, X., Wang, L., 2022. Biomineralized synthesis of palladium nanoflowers for photothermal treatment of cancer and wound healing. Int. J. Pharm. 615, 121489. https://doi.org/10.1016/j.ijpharm.2022.121489

Hosny, M., Fawzy, M., 2021. Instantaneous phytosynthesis of gold nanoparticles via persicaria salicifolia leaf extract, and their medical applications. Adv. Powder Technol. 32, 2891-2904. https://doi.org/10.1016/j.apt.2021.06.004

Huang, Y., Guo, X., Wu, Y., Chen, X., Feng, L., Xie, N., Shen, G., 2024. Nanotechnology's frontier in combatting infectious and inflammatory diseases: Prevention and treatment. Sig Transduct Target Ther. 9. https://doi.org/10.1038/s41392-024-01745-z

Ghareib, M., Abu Tahon, M., Abdallah, W.E., Hussein, M., 2019. Free radical scavenging activity of zinc oxide nanoparticles biosynthesised using *Aspergillus carneus*. Micro Nano Lett. 14, 1157-1162. https://doi.org/10.1049/mnl.2019.0218

Gholami-Shabani, M., Sotoodehnejadnematalahi, F., Shams-Ghahfarokhi, M., Eslamifar, A., Razzaghi-Abyaneh, M., 2023. Platinum nanoparticles as potent anticancer and antimicrobial agent: Green synthesis, physical characterization, and in-vitro biological activity. J. Clust. Sci. 34, 501-516. https://doi.org/10.1007/s10876-022-02225-6

Ibne Shoukani, H., Nisa, S., Bibi, Y., Zia, M., Sajjad, A., Ishfaq, A., Ali, H., 2024. Ciprofloxacin loaded PEG coated znO nanoparticles with enhanced antibacterial and wound healing effects. Sci. Rep. 14, 4689. https://doi.org/10.1038/s41598-024-55306-z

Issaka, E., Wariboko, M.A., Agyekum, E.A., 2024. Synergy and coordination between biomimetic nanoparticles and biological cells/Tissues/Organs/Systems: Applications in nanomedicine and prospect. Biomed. Mater. Devices 2, 1-33. https://doi.org/10.1007/s44174-023-00084-x

Jayakumar, T., Mani, G., Dhayalan, S., Sennimalai, R., Krishnamoorthy, K., Govindasamy, C., Al-Numair, K.S., Alsaif, M.A., Cheon, Y.P., 2023. Characterization, antimicrobial and anticancer properties of palladium nanoparticles biosynthesized routed through bacillus sp. J. Clust. Sci. 34, 2919-2930. https://doi.org/10.1007/s10876-023-02435-6

Jayamani, T., Arul Prasad T, A., Edal Queen, J., Scholastica Mary Vithiya, B., Tamizhdurai, P., Siva Kumar, N., Al-Fatesh, A.S., Reddy Koduru, J., 2023. Catalytic reduction of anionic and cationic toxic dyes and evaluation of antimicrobial activity using green synthesized palladium nanoparticles employing carica papaya aqueous leaf extract. J. Saudi Chem. Soc. 27, 101759. https://doi.org/10.1016/j.jscs.2023.101759

Joshi, N.C., Negi, P.B., Gururani, P., 2024. A review on metal/metal oxide nanoparticles in food processing and packaging. Food Sci. Biotechnol. 33, 1307-1322. https://doi.org/10.1007/s10068-023-01500-0

Karunakaran, G., Sudha, K.G., Ali, S., Cho, E.B., 2023. Biosynthesis of nanoparticles from various biological sources and its biomedical applications. Molecules 28, 4527. https://doi.org/10.3390/molecules28114527

Khairy, T., Amin, D.H., Salama, H.M., Elkholy, I.M.A., Elnakib, M., Gebreel, H.M., Sayed, H.A.E., 2024. Antibacterial activity of green synthesized copper oxide nanoparticles against multidrug-resistant bacteria. Sci. Rep. 14, 25020. https://doi.org/10.1038/s41598-024-75147-0

Khan, S., Rauf, A., Aljohani, A.S.M., Al-Awthan, Y.S., Ahmad, Z., Bahattab, O.S., Khan, S., Saadiq, M., Khan, S.A., Thiruvengadam, R., Thiruvengadam, M., 2024. Green synthesis of silver and gold nanoparticles in callistemon viminalis extracts and their antimicrobial activities. Bioprocess Biosyst. Eng. 47, 1197-1211. https://doi.org/10.1007/s00449-024-02994-6

Khosravi, A., Khamari D., 2019. Palladium nanoparticles stimulate keratinocyte proliferation and migration while enhancing angiogenesis and collagen synthesis through VEGF signaling in wound healing. Nanomedicine. Nanotechnol. Biol. Med. 15.

Khuda, F., Ul Haq, Z., Ilahi, I., Ullah, R., Khan, A., Fouad, H., Ali Khan Khalil, A., Ullah, Z., Umar Khayam Sahibzada, M., Shah, Y., Abbas, M., Iftikhar, T., El-Saber Batiha, G., 2021. Synthesis of gold nanoparticles using sambucus wightiana extract and investigation of its antimicrobial, anti-inflammatory, antioxidant and analgesic activities. Arab. J. Chem. 14, 103343. https://doi.org/10.1016/j.arabjc.2021.103343

Kumalasari, M.R., Alfanaar, R., Andreani, A.S., 2024. Gold nanoparticles (AuNPs): A versatile material for biosensor application. Talanta Open 9, 100327. https://doi.org/10.1016/j.talo.2024.100327

Kumar, S., Sood, S., 2020. Palladium nanoparticles induce PI3K/Akt and MAPK signaling pathways in cancer cells. J. Nanobiotechnol. 18, 1-13. https://doi.org/10.1186/s12951-020-06090-6

Kumari, S., Raturi, S., Kulshrestha, S., Chauhan, K., Dhingra, S., András, K.ács, Thu, K., Khargotra, R., Singh, T., 2023. A comprehensive review on various techniques used for synthesizing nanoparticles. J. Mater. Res. Technol. 27, 1739-1763. https://doi.org/10.1016/j.jmrt.2023.09.291

Kuniyil, M., Kumar, J.V.S., Adil, S.F., Shaik, M.R., Khan, M., Assal, M.E., Siddiqui, M.R.H., Al-Warthan, A., 2019. One-pot synthesized pd@N-doped graphene: An efficient catalyst for suzuki–Miyaura couplings. Catalysts 9, 469. https://doi.org/10.3390/catal9050469

Li, N., Mahdavi, B., Baghayeri, M., 2024. Green preparation of pd nanoparticles for treatment of gastric cancer and electrochemical sensing of bisphenol A in food. Food Meas. 18, 955-961. https://doi.org/10.1007/s11694-023-02255-2

Lin, G., Zhang, Z., Ju, Q., Wu, T., Segre, C.U., Chen, W., Peng, H., Zhang, H., Liu, Q., Liu, Z., Zhang, Y., Kong, S., Mao, Y., Zhao, W., Suenaga, K., Huang, F., Wang, J., 2023. Bottom-up evolution of perovskite clusters into high-activity rhodium nanoparticles toward alkaline hydrogen evolution. Nat. Commun. 14, 280. https://doi.org/10.1038/s41467-023-35783-y

Liu, C., Yu, Y., Fang, L., Wang, J., Sun, C., Li, H., Zhuang, J., Sun, C., 2024. Plant-derived nanoparticles and plant virus nanoparticles: Bioactivity, health management, and delivery potential. Crit. Rev. Food Sci. Nutr. 64, 8875-8891. https://doi.org/10.1080/10408398.2023.2204375

Liu, J., Zheng, X., 2017. Palladium nanoparticles: Recyclable catalysts and their applications in therapeutic treatments. Adv. Drug Deliv. Rev. 113, 47-62. https://doi.org/10.1016/j.addr.2017.04.001

Liu, Y., Li, J., Chen, M., Chen, X., Zheng, N., 2020. Palladium-based nanomaterials for cancer imaging and therapy. Theranostics 10, 10057-10074. https://doi.org/10.7150/thno.45990

Losada-Garcia, N., Santos, A.S., Marques, M.M.B., Palomo, J.M., 2023. Temperature-induced formation of pd nanoparticles in heterogeneous nanobiohybrids: Application in c–H activation catalysis. Nanoscale Adv. 5, 513-521. https://doi.org/10.1039/d2na00742h

Manasa, D.J., Chandrashekar, K..R., Pavan Kumar, M..A., Suresh, D., Madhu Kumar, D..J., Ravikumar, C.R., Bhattacharya, T., Ananda Murthy, H..C., 2021. Proficient synthesis of zinc oxide nanoparticles from tabernaemontana heyneana wall. via green combustion method: Antioxidant, anti-inflammatory, antidiabetic, anticancer and photocatalytic activities. Results Chem. 3, 100178. https://doi.org/10.1016/j.rechem.2021.100178

Meena, J., Sivasubramaniam, S.shankari, David, E., K, S., 2024. Green supercapacitors: Review and perspectives on sustainable template-free synthesis of metal and metal oxide nanoparticles. RSC Sustain. 2, 1224-1245. https://doi.org/10.1039/d4su00009a

MubarakAli, D., Kim, H., Venkatesh, P.S., Kim, J.W., Lee, S.Y., 2023. A systemic review on the synthesis, characterization, and applications of palladium nanoparticles in biomedicine. Appl. Biochem. Biotechnol. 195, 3699-3718. https://doi.org/10.1007/s12010-022-03840-9

Nandhini, J., Karthikeyan, E., Sheela, M., Bellarmin, M., Gokula Kannan, B., Pavithra, A., Sowmya Sri, D., Siva Prakash, S., Rajesh Kumar, S., 2025. Optimization of microwave-assisted green synthesis of zinc oxide nanoparticles using ocimum americanum and euphorbia hirta extracts: In vitro evaluation of antioxidant, anti-inflammatory, antibacterial, cytotoxicity, and wound healing properties. Intelligent Pharmacy 3, 90-109. https://doi.org/10.1016/j.ipha.2024.09.003

Naser, S.S., Gupta, A., Choudhury, A., Yadav, A., Sinha, A., Kirti, A., Singh, D., Kujawska, M., Kaushik, N.K., Ghosh, A., De, S., Verma, S.K., 2024. Biophysical translational paradigm of polymeric nanoparticle: Embarked advancement to brain tumor therapy. Biomed. Pharmacother. 179, 117372. https://doi.org/10.1016/j.biopha.2024.117372

Nie, L., Chen, M., Sun, X., Rong, P., Zheng, N., Chen, X., 2014. Palladium nanosheets as highly stable and effective contrast agents for in vivo photoacoustic molecular imaging. Nanoscale 6, 1271-1276. https://doi.org/10.1039/c3nr05468c

Nizar Ahamed, A., Mohamed Yaser, S., Mohammad Idhris, S., Syed Ali Padusha, M., Ahamed Sherif, N., 2023. Phytochemical and pharmacological potential of the genus plectranthus—A review. S. Afr. J. Bot. 154, 159-189. https://doi.org/10.1016/j.sajb.2023.01.026

Adeyemi, J.O., Oriola, A.O., Onwudiwe, D.C., Oyedeji, A.O., 2022. Plant extracts mediated metal-based nanoparticles: Synthesis and biological applications. Biomolecules 12, 627. https://doi.org/10.3390/biom12050627

Orzari, L.O.ávio, Silva, L.R.G.e, de Freitas, R.C., Brazaca, L.ísC., Janegitz, B.C., 2024. Lab-made disposable screen-printed electrochemical sensors and immunosensors modified with pd nanoparticles for parkinson's disease diagnostics. Microchim. Acta 191. https://doi.org/10.1007/s00604-023-06158-3

Palliyarayil, A., Prakash, P.S., Nandakumar, S., Kumar, N.S., Sil, S., 2020. Palladium nanoparticles impregnated activated carbon material for catalytic oxidation of carbon monoxide. Diam. Relat. Mater. 107, 107884. https://doi.org/10.1016/j.diamond.2020.107884

Panda, P.K., Verma, S.K., Suar, M., 2021. Nanoparticle-biological interactions: The renaissance of bionomics in the myriad nanomedical technologies. Nanomedicine (Lond) 16, 2249-2254. https://doi.org/10.2217/nnm-2021-0174

Paramasivam, D., Balasubramanian, B., Park, S., Alagappan, P., Kaul, T., Liu, W. and Pachiappan, P., 2020. Phytochemical profiling and biological activity of plectranthus amboinicus (Lour.) mediated by various solvent extracts against aedes aegypti larvae and toxicity evaluation. Asian Pac. J. Trop. Med. 13, 494. https://doi.org/10.4103/1995-7645.295360

Paul, P., Verma, S.K., Kumar Panda, P., Jaiswal, S., Sahu, B.R., Suar, M., 2018. Molecular insight to influential role of hha–TomB toxin–antitoxin system for antibacterial activity of biogenic silver nanoparticles. Artif. Cells Nanomed. Biotechnol. 46, 572-584. https://doi.org/10.1080/21691401.2018.1503598

Phuong, T.D.V., Trang, N.T.K., Tam, P.D., 2024. Electrochemical behavior of palladium nanoparticles deposition on glassy carbon electrode from reline and ethaline and its application in DNA sensors. J. Solid State Electrochem. 28, 2777-2786. https://doi.org/10.1007/s10008-024-05844-3

Puri, A., Mohite, P., Maitra, S., Subramaniyan, V., Kumarasamy, V., Uti, D.E., Sayed, A.A., El-Demerdash, F.M., Algahtani, M., El-Kott, A.F., Shati, A.A., Albaik, M., Abdel-Daim, M.M., Atangwho, I.J., 2024. From nature to nanotechnology: The interplay of traditional medicine, green chemistry, and biogenic metallic phytonanoparticles in modern healthcare innovation and sustainability. Biomed. Pharmacother. 170, 116083. https://doi.org/10.1016/j.biopha.2023.116083

Rai, M., Yadav, A., Gade, A., 2009. Silver nanoparticles as a new generation of antimicrobials. Biotechnol. Adv. 27, 76-83. https://doi.org/10.1016/j.biotechadv.2008.09.002

Rehman, H., Ali, W., Zaman Khan, N., Aasim, M., Khan, T., Ali Khan, A., 2023. Delphinium uncinatum mediated biosynthesis of zinc oxide nanoparticles and in-vitro evaluation of their antioxidant, cytotoxic, antimicrobial, anti-diabetic, anti-inflammatory, and anti-aging activities. Saudi J. Biol. Sci. 30, 103485. https://doi.org/10.1016/j.sjbs.2022.103485

Rehman, G., Umar, M., Shah, N., Hamayun, M., Ali, A., Khan, W., Khan, A., Ahmad, S., Alrefaei, A.F., Almutairi, M.H., Moon, Y.S., Ali, S., 2023. Green synthesis and characterization of silver nanoparticles using azadirachta indica seeds extract: In vitro and in vivo evaluation of anti-diabetic activity. Pharmaceuticals (Basel) 16, 1677. https://doi.org/10.3390/ph16121677

Rokkarukala, S., Cherian, T., Ragavendran, C., Mohanraju, R., Kamaraj, C., Almoshari, Y., Albariqi, A., Sultan, M.H., Alsalhi, A., Mohan, S., 2023. One-pot green synthesis of gold nanoparticles using sarcophyton crassocaule, a marine soft coral: Assessing biological potentialities of antibacterial, antioxidant, anti-diabetic and catalytic degradation of toxic organic pollutants. Heliyon 9, e14668. https://doi.org/10.1016/j.heliyon.2023.e14668

Sadalage, P.S., Pawar, K.D., 2023. Adsorption and removal of ethidium bromide from aqueous solution using optimized biogenic catalytically active antibacterial palladium nanoparticles. Environ. Sci. Pollut. Res. Int. 30, 5005-5026. https://doi.org/10.1007/s11356-022-22526-7

Saleh, T.A., Fadillah, G., 2023. Green synthesis protocols, toxicity, and recent progress in nanomaterial-based for environmental chemical sensors applications. Trends Environ. Anal. Chem. 39, e00204. https://doi.org/10.1016/j.teac.2023.e00204

Sandhya, K., Bhagavanth Reddy, G., Ayodhya, D., Venkatesh, B., Kondaiah, S., Noorjahan, M., Yadagiri Swamy, P., Girija Mangatayaru, K., 2024. Ultrasound assisted biogenic synthesis of palladium nanoparticles using cocculus hirsutus leaf extract: Antimicrobial, anti-inflammatory and catalytic activities. J. Mol. Struct. 1306, 137848. https://doi.org/10.1016/j.molstruc.2024.137848

Sarmah, M., Neog, A.B., Boruah, P.K., Das, M.R., Bharali, P., Bora, U., 2019. Effect of substrates on catalytic activity of biogenic palladium nanoparticles in c-C cross-coupling reactions. ACS Omega 4, 3329-3340. https://doi.org/10.1021/acsomega.8b02697

Seku, K., Pejjai, B., Osman, A.I., Hussaini, S.S., Al Abri, M., Kumar, N.S., Vijaya Kumar, N.S., Reddy, S.S.K., Sadasivuni, K.K., Al Fatesh, A.S., Reddy, B., 2024. Ecofriendly synthesis of Salmalia Malabarica gum stabilized palladium nanoparticles: antibacterial and catalytic properties. Biomass Convers. Biorefinery. https://doi.org/10.1007/s13399-024-05443-2

Shahid-ul-Islam, , Bairagi, S., Kamali, M.R., 2023. Review on green biomass-synthesized metallic nanoparticles and composites and their photocatalytic water purification applications: Progress and perspectives. Chem. Eng. J. Adv. 14, 100460. https://doi.org/10.1016/j.ceja.2023.100460

Shanthi, K., Vimala, K., Gopi, D., Kannan, S., 2015. Fabrication of a pH responsive DOX conjugated PEGylated palladium nanoparticle mediated drug delivery system: An in vitro and in vivo evaluation. RSC Adv. 5, 44998-45014. https://doi.org/10.1039/c5ra05803a

Sharifi-Rad, M., Pohl, P., Epifano, F., Álvarez-Suarez, J.M., 2020. Green synthesis of silver nanoparticles using astragalus tribuloides delile Root extract: Characterization, antioxidant, antibacterial, and anti-inflammatory activities. Nanomaterials (Basel) 10, 2383. https://doi.org/10.3390/nano10122383

Shokouhimehr, M., Yek, S.M.-G., Nasrollahzadeh, M., Kim, A., Varma, R.S., 2019. Palladium nanocatalysts on hydroxyapatite: Green oxidation of alcohols and reduction of nitroarenes in water. Appl. Sci. 9, 4183. https://doi.org/10.3390/app9194183

Shukla, F., Patel, M., Gulamnabi, Q., Thakore, S., 2023. Palladium nanoparticles-confined pore-engineered urethane-linked thiol-functionalized covalent organic frameworks: A high-performance catalyst for the suzuki miyaura cross-coupling reaction. Dalton Trans. 52, 2518-2532. https://doi.org/10.1039/d2dt04057c

Skłodowski, K., Chmielewska-Deptuła, S.J., Piktel, E., Wolak, P., Wollny, T., Bucki, R., 2023. Metallic nanosystems in the development of antimicrobial strategies with high antimicrobial activity and high biocompatibility. Int. J. Mol. Sci. 24, 2104. https://doi.org/10.3390/ijms24032104

Soliman, W.E., Elsewedy, H.S., Younis, N.S., Shinu, P., Elsawy, L.E., Ramadan, H.A., 2022. Evaluating antimicrobial activity and wound healing effect of rod-shaped nanoparticles. Polymers (Basel) 14, 2637. https://doi.org/10.3390/polym14132637

Solomon, N.O., Kanchan, S., Kesheri, M., 2024. Nanoparticles as detoxifiers for industrial wastewater. Water. Air. Soil Pollut. 235. https://doi.org/10.1007/s11270-024-07016-5

Sreejith, L., Soniya, E.V., Madhusudanan, K.P., 2016. Cerium oxide nanoparticles as redox modulators and angiogenesis activators: Implications for wound healing and tissue regeneration. J. Nanosci. Nanotechnol. 16, 367-374.

Tahir, K., Nazir, S., Li, B., Ahmad, A., Nasir, T., Khan, A.U., Shah, S.A., Khan, Z.U., Yasin, G., Hameed, M.U., 2016. Sapium sebiferum leaf extract mediated synthesis of palladium nanoparticles and in vitro investigation of their bacterial and photocatalytic activities. J. Photochem. Photobiol. B. 164, 164-173. https://doi.org/10.1016/j.jphotobiol.2016.09.030

Tiri, R.N.E., Aygun, A., Bekmezci, M., Gonca, S., Ozdemir, S., Kaymak, G., Karimi-Maleh, H., Sen, F., 2024. Environmental energy production and wastewater treatment using synthesized pd nanoparticles with biological and photocatalytic activity. Top. Catal. 67, 714-724. https://doi.org/10.1007/s11244-024-01912-0

Todaria, M., Maity, D., Awasthi, R., 2024. Biogenic metallic nanoparticles as game-changers in targeted cancer therapy: Recent innovations and prospects. Futur. J. Pharm. Sci. 10. https://doi.org/10.1186/s43094-024-00601-9

Verma, S.K., Jha, E., Kiran, K..J., Bhat, S., Suar, M., Mohanty, P.S., 2016. Synthesis and characterization of novel polymer-hybrid silver nanoparticles and its biomedical study. Mater. Today: Proc. 3, 1949-1957. https://doi.org/10.1016/j.matpr.2016.04.096

Verma, S.K., Jha, E., Panda, P.K., Thirumurugan, A., Suar, M.. Biological effects of green-synthesized metal nanoparticles: A mechanistic view of antibacterial activity and cytotoxicity. In: Naushad, M., Rajendran, S., Gracia, F. (eds) Advanced Nanostructured Materials for Environmental Remediation. Environmental Chemistry for a Sustainable World, vol 25. Springer, Cham. https://doi.org/10.1007/978-3-030-04477-0_6

Verma, S.K., Suar, M., Mishra, Y.K., 2022. Editorial: Green perspective of nano-biotechnology: Nanotoxicity horizon to biomedical applications. Front Bioeng. Biotechnol. 10, 919226. https://doi.org/10.3389/fbioe.2022.919226

Vijayaram, S., Razafindralambo, H., Sun, Y.-Z., Vasantharaj, S., Ghafarifarsani, H., Hoseinifar, S.H., Raeeszadeh, M., 2024. Applications of green synthesized metal nanoparticles — a review. Biol. Trace Elem. Res. 202, 360-386. https://doi.org/10.1007/s12011-023-03645-9

Vijwani, H., Agrawal, A., Mukhopadhyay, S.M., 2012. Dechlorination of environmental contaminants using a hybrid nanocatalyst: Palladium nanoparticles supported on hierarchical carbon nanostructures. J. Nanotechnol. 2012, 1-9. https://doi.org/10.1155/2012/478381

Vinnacombe-Willson, G.A., Conti, Y., Stefancu, A., Weiss, P.S., Cortés, E., Scarabelli, L., 2023. Direct bottom-up in situ growth: A paradigm shift for studies in wet-chemical synthesis of gold nanoparticles. Chem. Rev. 123, 8488-8529. https://doi.org/10.1021/acs.chemrev.2c00914

Wang, Y.L., Tan, D.X., Zhang, H.Y., Chen, S., Bian, L., 2015. Synthesis, characterization, and electrocatalytic properties of 3D aggregates of palladium nanocrystallites. Mater. Res. Innovations 19, 196-203. https://doi.org/10.1179/1433075x14y.0000000242

Williams, L.A.D., Vasquez, E.A., Milan, P.P., Zebitz, C., Kraus, W.. In vitro anti-inflammatory and antimicrobial activities of phenylpropanoids from piper betle l. (Piperaceae). In: Rauter, A.P., Palma, F.B., Justino, J., Araújo, M.E., dos Santos, S.P. (eds) Natural Products in the New Millennium: Prospects and Industrial Application. Proceedings of the Phytochemical Society of Europe, vol 47. Springer, Dordrecht. https://doi.org/10.1007/978-94-015-9876-7_22

Yin, X., Fan, T., Zheng, N., Yang, J., Yan, L., He, S., Ai, F., Hu, J., 2023. Palladium nanoparticle based smart hydrogels for NIR light-triggered photothermal/photodynamic therapy and drug release with wound healing capability. Nanoscale Adv. 5, 1729-1739. https://doi.org/10.1039/d2na00897a

Zare-Bidaki, M., Ghasempour, A., Mohammadparast-Tabas, P., Ghoreishi, S.M., Alamzadeh, E., Javanshir, R., Le, B.N., Barakchi, M., Fattahi, M., Mortazavi-Derazkola, S., 2023. Enhanced in vivo wound healing efficacy and excellent antibacterial, antifungal, antioxidant and anticancer activities via agNPs@PCS. Arab. J. Chem. 16, 105194. https://doi.org/10.1016/j.arabjc.2023.105194

Zhang, L., Wang, H., 2017. The role of DMSO as a vehicle control in experimental wound healing studies. J. Wound Care, 26, 389-396.

Zhang, X., Liu, Y., 2019. Palladium nanoparticles in wound healing applications: Catalytic properties and ROS modulation for therapeutic effects. J. Nanomed. 15, 72-80.

Zheng, J., Zhang, H., Xu, T., Ju, S., Xia, G., Yu, X., 2024. Copper and cobalt nanoparticles enable highly stable and fast kinetics of al–S batteries. Adv. Funct. Materials 34. https://doi.org/10.1002/adfm.202307486

Zheng, Q., Chen, C., Liu, Y., Gao, J., Li, L., Yin, C., Yuan, X., 2024. Metal nanoparticles: Advanced and promising technology in diabetic wound therapy. Int. J. Nanomedicine 19, 965-992. https://doi.org/10.2147/IJN.S434693